Agricultural and Forest Meteorology 271 (2019) 398–412

Contents lists available at ScienceDirect

Agricultural and Forest Meteorology

journal homepage: www.elsevier.com/locate/agrformet

Closure and partitioning of the energy balance in a preserved area of a Brazilian seasonally dry tropical forest

Suany Campos[a,*], Keila R. Mendes[a], Lindenberg L. da Silva[b], Pedro R. Mutti[a], Salomão S. Medeiros[c], Laerte B. Amorim[d], Carlos A.C. dos Santos[b,e], Aldrin M. Perez-Marin[c], Tarsila M. Ramos[f], Thiago V. Marques[a], Paulo S. Lucio[a,f], Gabriel B. Costa[g], Cláudio M. Santos e Silva[a,f], Bergson G. Bezerra[a,f]

[a] Climate Sciences Post-graduate Program, Federal University of Rio Grande do Norte, Av. Senador Salgado Filho, 3000, 59078-970, Lagoa Nova, Natal, Brazil
[b] Meteorology Post-graduate Program, Federal University of Campina Grande, Rua Aprígio Veloso, 882, 58429-900, Universitário, Campina Grande, Brazil
[c] National Institute of Semi-Arid, Av. Francisco Lopes de Almeida, s/n, 58434-700, Serrotão, Campina Grande, Brazil
[d] Federal Institute of Education, Science and Thecnology of Piauí, Estr. p/ Wall Ferraz, s/n, 64500-000, Uberaba II, Oeiras, Brazil
[e] Academic Unit of Atmospheric Sciences, Federal University of Campina Grande, Rua Aprígio Veloso, 882, 58429-900, Universitário, Campina Grande, Brazil
[f] Department of Atmospheric and Climate Sciences, Federal University of Rio Grande do Norte, Av. Senador Salgado Filho, 3000, 59078-970, Lagoa Nova, Natal, Brazil
[g] Federal University of Western Pará, Av. Mendonça Furtado, 2440, 68040-050, Aldeia, Santarém, Brazil

ARTICLE INFO

Keywords:
SDTF
Caatinga biome
Eddy covariance
Energy balance closure
Energy partitioning

ABSTRACT

The energy balance closure obtained through the eddy covariance method is a problem which persists, despite advances in the development and improvement of instruments and recent efforts in the description of corrections and in the characterization of measuring uncertainties. In most places the sum of sensible and latent heat fluxes (H and λE) is less than available energy, i.e. the difference between net radiation (Rn) and soil heat flux (G). This study analyzed the annual and seasonal behavior of the energy partitioning and energy balance closure in the Caatinga Biome, which is a seasonally dry tropical forest located in the semiarid lands of Brazil, using the eddy covariance method. Results showed high seasonal variability in the energy partitioning. During the dry season, approximately 70% of Rn was converted into H and less than 5% of it was converted into latent heat flux (λE). During the wet season, the Rn portion converted into H and λE was similar: ˜ 40%. In annual terms, the Rn portion converted into H and λE was of the order of 50% and 20% respectively. The degree of the energy balance closure varied depending on the method used. When the closure was calculated using orthogonal regressions, the slope varied from 0.87 to 0.90 in 2014 and from 0.92 to 1.00 in 2015. However, when the closure was calculated by the energy balance ratio method, values varied from 0.70 to 0.79 in 2014 and from 0.73 to 0.82 in 2015. The closure was better in 2015 if compared to 2014 possibly due to the more intense turbulence observed in 2015 because friction velocity was higher than in 2014. The better closure in 2015 may also be associated with large eddies, which were more frequent in 2014 as evidenced by the correction coefficients for vertical wind velocity and water vapor and vertical wind velocity and sonic temperature. The energy balance closure was also analyzed considering atmospheric instability conditions and the best results were found under very unstable conditions, while the least expressive results were found under stable conditions. Under these conditions negative values of the energy balance ratio were also observed during dry and transition seasons, indicating that fluxes were reversed during these periods.

1. Introduction

Seasonally Dry Tropical Forests (SDTF) occupy wide areas in the tropical regions of most continents which have dry seasons (defined as the number of months with rainfall ≤ 100 mm) with a duration of up to six uninterrupted months (Murphy and Lugo, 1986; Allen et al., 2017; del Castillo et al., 2018). In the Neotropics, these forests are found surrounding the Amazon basin and extending north towards Mexico and the Caribbean (Linares-Palomino et al., 2011; Banda-R et al., 2016; Santos et al., 2012). Despite their wide distribution in South America, most of the SDTF occur as isolated patches. The only exception is the Caatinga Biome (Northeast of Brazil), in which there is a functional

* Corresponding author.
E-mail address: suanyfis05@gmail.com (S. Campos).

https://doi.org/10.1016/j.agrformet.2019.03.018
Received 28 December 2018; Received in revised form 19 March 2019; Accepted 21 March 2019

ecosystem covering an area of approximately 800,000 km^2 (Santos et al., 2012; Koch et al., 2017). In addition, this biome has been identified as one of the most important wildlife areas of the planet and one of its most biodiverse and highly endemic dry forests (Mittermeier et al., 2003; Pennington et al., 2006; Holzman, 2008; Santos et al., 2014; Koch et al., 2017).

The Caatinga is characterized as a deciduous thorny savannah (Tsuchiya, 1995). Its natural environment, the Brazilian Semiarid, has a mean temperature of 25 °C with little variability throughout the year. Mean annual rainfall ranges from 300 mm to 1000 mm, concentrated mostly in a 3–4 months period (during summer and autumn), followed by an extended dry season lasting from 8 to 9 months (between winter and spring) (Pagoto et al., 2015; Oliveira et al., 2017). On the other hand, potential evapotranspiration rates are high (between 1500 and 2000 mm^{-1} year) and the soil is shallow and rocky, with a reduced capacity for water absorption (Pagoto et al., 2015).

Reports by the Brazilian Panel on Climate Change (PBMC, 2014) project an increase of 0.5° to 1 °C in air temperature and a decrease between 10% and 20% in rainfall rates in the Caatinga during the next three decades (2020–2040). Furthermore, temperature is expected to gradually increase by 1.5° to 2.5 °C in the 2041–2070 period while rainfall rates are expected to decrease by 25% and 35% in the same period. These projections suggest that by the end of the 21 st century the Caatinga Biome will be considerably more arid, with the occurrence of longer droughts and more severe water shortage, exposing its biodiversity to a potentially catastrophic risk (PBMC, 2014; Marengo and Bernasconi, 2015).

Given this scenario, the following questions arise: is the Caatinga Biome tolerant to a more arid, warmer environment? What is the threshold of increasing aridity and warming to which Caatinga species can tolerate? According to the scientific literature, the answers to these questions are still unclear (Santos et al., 2014; Allen et al., 2017). These knowledge gaps exist due to the uncertainty of the scientific knowledge that has been generated about SDTF, as reported by Dombroski et al. (2011) and Koch et al. (2017).

Terrestrial ecosystems play an important role in the global cycle of carbon dioxide, as they are considered CO_2 sinks. Because of that, they are key elements in the mitigation of the effects of climate change (Schimel et al., 2001; Luyssaert et al., 2007; Beer et al., 2010). Therefore, it is of the uttermost importance to investigate water vapour exchange mechanisms and the physical processes associated with the energy balance in a variety of terrestrial ecosystems, in order to better understand their functioning and the feedbacks (Pielke et al., 1998) that control the CO_2 cycle (Baldocchi et al., 2004; Hao et al., 2007) and their relationship with climate change (Foley et al., 2003). Thus, measurements of heat and mass exchanges in ecosystem-atmosphere interactions are crucial for understanding the dynamics of the climate system, as well as for evaluating dynamical climate models (Jaeger et al., 2009) and validating energy fluxes estimated by remote sensing (Xu et al., 2017).

There is a shortage of scientific studies concerning energy and carbon balances in the Caatinga Biome, in such a way that it is difficult to estimate its impact in regional and global CO_2 balance. Studies with this purpose in the Caatinga are still incipient despite some recent advances (Teixeira et al., 2008; Souza et al., 2016; Pires et al., 2017; Silva et al., 2017) in the State of Pernambuco, in areas of preserved or in-recovery vegetation during years of below-average rainfall. In Brazil, such studies have been carried out in different biomes, such as the transition zone between the savanna and the Amazon forest, rainforests and pastures, the Cerrado, wetlands (Pantanal Biome) and eucalyptus forests (Vourlitis et al., 2001; da Rocha et al., 2009; Cabral et al., 2010; von Randow et al., 2004; 2013; Cabral et al., 2015; Biudes et al., 2015). However, as noted, most of these studies were carried out in the Amazon region (da Rocha et al., 2004; Sotta et al., 2007; Meir et al., 2008; Araújo et al., 2010; Metcalfe et al., 2010. Zeri et al., 2014). The eddy covariance technique (EC) is the most widely used method in the scientific literature to determine mass and heat fluxes in the soil-vegetation-atmosphere interface (Baldocchi et al., 2001; Baldocchi, 2008). Despite the generally good reliability of the EC method, there is usually an incongruity between the sum of eddy fluxes of sensible and latent heat ($H + \lambda E$) and the sum of the available energy (net radiation minus soil heat flux), where the difference between these sums can vary from 10% to 30%, resulting in the non-closure of the energy balance (Wilson et al., 2002; Foken, 2008; Leuning et al., 2012). According to McGloin et al. (2018), the energy balance closure (EBC) directly affects the evaluation of λE and H, and it is also potentially relevant to the interpretation of other fluxes, such as CO_2 (Wilson et al., 2002; Barr et al., 2006). Thus, the lack of EBC incurs in important implications when estimating energy, water and carbon budgets using EC flux measurements.

According to Gerken et al. (2018), despite recent efforts such as research in developing the fundamental equations for eddy covariance, developing and improving instruments, describing corrections, and characterizing measurement uncertainty (e.g., Massman and Lee, 2002; Moncrieff et al., 2005; Papale et al., 2006; Gu et al., 2012; Leuning et al., 2012) the energy imbalance problem still persists on all types of surfaces.

The lack of EBC might be explained by several reasons. Some errors may result in the overestimation of the available energy, while others incur in the underestimation of turbulent fluxes (Wilson et al., 2002; McGloin et al., 2018). According to Foken (2008), possible reasons for the overestimation of the available energy could be the overestimation of Rn and erroneous quantification of the energy stored in the soil, in the air below the tower or in the vegetation. However, with the improvement in the accuracy of radiometers it is unlikely that Rn measurement errors are the main cause of the EBC problem.

According to Leuning et al. (2012), precise measurements of available energy require net radiation data and soil, air and biomass heat storage data for each half-hourly average period, which is the time interval typically used by the scientific community for the measurement of fluxes. Phase lags caused by incorrect estimates of the storage terms are considered one of the important reasons why the sum of sensible and latent heat fluxes systematically underestimates available energy at this time scale.

Another possible explanation for the lack of EBC is the occurrence of low frequency turbulence that is not captured by the EC system (Eder et al., 2014; McGloin et al., 2018; Stoy et al., 2013). Recently, the effect of phase differences between vertical wind velocity and water vapor in the energy balance closure has been studied (Gao et al., 2017; McGloin et al., 2018).

Considering the importance of research on the energy balance between terrestrial ecosystems and the atmosphere, as well as the shortage of this type of study in the Caatinga Biome, the present research provides an analysis of the annual and seasonal behavior of the energy balance closure and partitioning in a preserved Brazilian semiarid Caatinga forest. Additionally, it aims to analyze the relationship between EBC, friction velocity and the stability parameter.

2. Material and method

2.1. Study area

The study was conducted in a preserved fragment of a seasonally dry tropical forest, the Caatinga Biome, in the Semiarid of the Northeast Brazil (6°34′42″S, 37°15′05″W, 205 m above sea level). A micrometeorological tower equipped with an EC system at a 11 m height was installed in a conservation unit of the Caatinga Biome, the Seridó Ecological Station (ESEC-Seridó), near the town of Serra Negra do Norte, in the Rio Grande do Norte State (Fig. 1). The area of the ESEC-Seridó is managed by the Chico Mendes Institute for Biodiversity Conservation (ICMBio). The micrometeorological tower belongs to the Brazilian National Institute of Semiarid (INSA) and is part of the

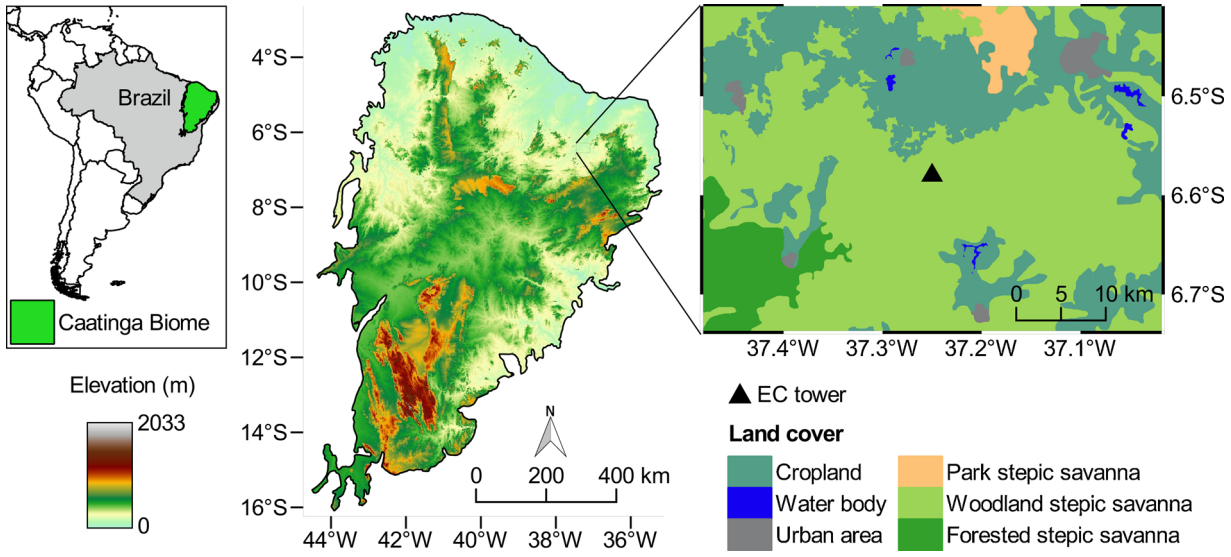

Fig. 1. Location of the Caatinga Biome in relation to South America and Brazil (left figure), elevation of the Caatinga Biome (mid figure), and land cover around the ESEC-Seridó (right figure).

National Observatory of Water and Carbon Dynamics in the Caatinga Biome (NOWCDCB) network.

The ESEC-Seridó comprises an area of 1163 ha of reminiscent Caatinga, characterized by dry xerophilous forest and deciduous plant species and the predominance of widely dispersed small trees and shrubs, with less than 7 m in height and herb patches, which develop and grow only during the wet season (Souza et al., 2012; Freitas et al., 2010; Althoff et al., 2016; Tavares-Damasceno et al., 2017). The predominant soil type is Litholic Neosol (Entisol in the North American classification), shallow (approximately 40 cm), stony and of low fertility (EMBRAPA, 2006; Althoff et al., 2016). The climate of the region is semiarid, Köppen's Bsh low longitude and altitude (Alvares et al., 2014), with the wet season occurring between the months of January and May, mean annual rainfall of 700.0 mm, mean annual temperature of 25.0 °C, and mean annual air humidity around 60% (30-yr mean) (INMET, 1992). The slope of the terrain ranges between 1–3 degrees.

2.2. Measurements and data

The field experiment was carried out from 01 January 2014 to 31 December 2015. Micrometeorological tower measurements provided two data sets: high frequency data from the EC measurements, and low frequency data. The high frequency data set consists of measurements of CO_2 and water vapor concentration, sonic temperature and the three wind components (u_x, u_y, u_z) obtained using an EC150 Open-Path CO_2/H_2O Gas Analyzer combined with the CSAT3A 3D Sonic Anemometer (Campbell Scientific, Inc., Logan, UT, USA). Since the EC150 is being used along with the sonic anemometer, they were installed pointing towards the predominant wind direction (southeast) in order to minimize flux distortions by the analyzer arms or by other support parts. Atmospheric pressure was measured using an *Enhanced Barometer PTB110* (Vaisala Corporation, Helsinki, Finland) while air temperature and relative humidity were measured using a HMP155 A probe (Vaisala Corporation, Helsinki, Finland). All these measurements were collected and stored at a 10 Hz frequency in a memory card attached to a CR3000 model *Datalogger* (Campbell Scientific, Inc., Logan, UT, USA).

The low frequency dataset includes net radiation and albedo, which were obtained by a CNR4 Net-radiometer (Kipp & Zonen, The Netherlands). Air temperature and relative humidity were measured using a HMP45C probe (Vaisala Corporation, Helsinki, Finland). All sensors were installed at 11.0 m of height above the surface, around 4.0 m above the trees in the site. Soil heat flux density (G, W m^{-2}) was obtained through the average value between the measurements of two model HFP01SC plates (Hukseflux Thermal Sensors, Delft, The Netherlands), installed at a depth of 0.05 m. The soil heat flux plates were installed in order to more faithfully represent the general land cover. Thus, installation directly under the tree canopy and in fully open areas was avoided. All data were sampled at a 5 s frequency and stored as half-hourly averages.

Meteorological conditions during the experiment were assessed through daily global radiation (Rg), air temperature (Ta) and vapour pressure deficit (VPD) values. The VPD is the difference between the saturation (e_s) and actual (e_a) vapor pressure. The method used for the calculation of VPD can be found in Allen et al. (1998).

2.3. Energy balance – closure and partitioning

The EB equation expresses the conversion of net energy into energy and mass fluxes between the canopy and the atmosphere. We neglected the energy stored in the canopy and the energy used in photosynthesis and respiration because they represent less than 2% of the net radiation (Heilman et al., 1994), especially in environments with lower canopy and leaf density, such as the Caatinga. However, observational evidence indicates that the EB equation produces a residual or deficit (Eq. (01)) which corresponds to the unmeasured metabolic terms, energy stored in the canopy, heat storage terms and differences between real radiation and turbulent fluxes versus their measured counterparts (Foken, 2008; Georg et al., 2016; Gerken et al., 2018; McGloin et al., 2018).

$$\varepsilon = Rn - \lambda E - H - G \quad (01)$$

where Rn is the net radiation, λE, H and G are the latent heat flux, sensible heat flux and soil heat flux densities, respectively, expressed in W m^{-2}. Usually ε is considerably larger than the 2% reported by Heilman et al. (1994).

The ε term is the EBC problem which was assessed using two methods. The first consisted in the calculation of orthogonal regression coefficients between half-hourly turbulent fluxes estimates ($\lambda E + H$, dependent variables) and the available energy ($Rn - G$, independent variables).

The second method used was the calculation of the bulk EBC fraction (hereinafter referred to as EBR), which is the ratio between the cumulative sums of $\lambda E + H$ and $Rn - G$ for each half-hour (Franssen et al., 2010; McGloin et al., 2018):

$$EBR = \frac{\sum(\lambda E + H)}{\sum(Rn - G)} \quad (02)$$

The dataset used in the EBR analysis consisted of intervals in which all half-hourly energy balance data were available or data with gaps that could be filled with the gap-filling procedure, which will be described in Section 2.4.

The EBR was analyzed in relation to the friction velocity (u_*) and the stability parameter (ξ). According to Gao et al. (2017) and McGloin et al. (2018), signals of vertical wind velocity and water vapor associated with large eddies (linked to entrainment and advection) result in an increase of ε. Thus, the relationships between the degree of EBR and the correction coefficients for vertical wind velocity and water vapor (R_{wq}) and vertical wind velocity and sonic temperature (R_{wT}) were analysed. The R_{wq} and R_{wT} correction coefficients were calculated through the following equations (Kaimal and Finnigan, 1994; McGloin et al., 2018):

$$R_{wq} = \frac{\overline{w'q'}}{\sigma_w \sigma_q} \quad (03)$$

$$R_{wT} = \frac{\overline{w'T'}}{\sigma_w \sigma_T} \quad (04)$$

where σ_w, σ_q and σ_T are the vertical wind velocity (m s $^{-1}$), water vapor (mmol m^{-3}) and sonic temperature (K) standard deviations and w', q' and T' are the turbulent components of the vertical wind velocity, water vapor and sonic temperature.

2.4. Data processing and post processing

For the retrieval of λE and H we used the LoggerNet (Campbell Scientific, Inc., Logan, UT, USA) software in order to transform 10 Hz raw data into 30 min binaries (TOB1). Afterwards, high frequency data were processed using the EdiRe software, transforming data into half-hourly averages. Data processing includes the detection of spikes, delay correction of H_2O/CO_2 in relation to the vertical wind component, coordinates correction (2D rotation) using the planar fit method, correction of spectral loss, sonic virtual temperature correction, corrections for flux density fluctuations (Webb et al., 1980), as well as the incorporated frequency response correction derived from Moore (1986) and Massman (2000). We also applied corrections regarding the reduction of wind velocity or the increase in turbulence caused by the shadow of the tower and the sensor. As the sensor was installed in order to remain pointed towards the predominant wind direction according to the equipment user guide (Campbell Scientific Inc., 2012), there were few data in the shadow zone direction.

For the detection of spurious data (spikes) we used a method described by Papale et al. (2006) based on the comparison between the difference of the 30 min flux value and the values immediately before and after it. This procedure was applied in an N = 60-day interval, using the median absolute deviation about the median (MAD).

Besides the careful maintenance and periodic calibration of the instruments, data were submitted to a rigorous post-processing procedure. The assessment of data quality was performed according to Mauder and Foken (2004) with indexes 0, 1 and 2 representing high-quality data (class 1), medium-quality data (class 2) and low-quality data (class 3), respectively. Only class 1 and 2 data were analyzed, while class 3 data (low-quality data) were discarded. Furthermore, data associated with the malfunctioning of the sensor and undeniably inconsistent data were rejected. After the application of all filtering criteria 77% of H and 64% of λE data were available for analysis. Thus, 23% of the H data was gap-filled, with 16% of nightime data and 7% of daytime data. On the other hand, 36% of the λE data was gap-filled, with 25% of nightime data and 11% of daytime data.

Gap filling due to data inconsistency and the rejection of spurious values was carried out by using the method described by Reichstein et al. (2005), which takes into consideration the covariance between fluxes and meteorological variables and also the temporal auto-correlation of fluxes. To fill the gaps we used an automated online tool provided by the Max Planck Institute.

2.5. Footprint calculation

The area in which fluxes were measured was evaluated through a footprint model developed by Kljun et al. (2015). The information required for the model are the height of flux measurement (z_m), the zero-plane displacement height (d), the surface friction velocity (u_*), the standard deviation of the vertical wind speed (σ_w) and the roughness length (z_0). According to Kljun et al. (2015) parameterization is valid for moderate friction velocity values ($u_* > 0{,}1\ m\ s^{-1}$) and for a limited range of boundary layer stability conditions ($-15{,}5 \leq z_m/L$), where L is the Monin-Obukhov length. For our study area we used $d = (2/3) \bullet h$ and $z_0 = 0.123 \bullet h$, where h is the canopy height, considered equal to 6 m.

2.6. Seasonal behavior of the Caatinga in response to rainfall

The seasonal behavior of the vegetation in response to rainfall was evaluated using NDVI (Normalized Difference Vegetation Index) data, computed from the red and near infrared reflectance values obtained by the MODIS (Moderate Resolution Imaging Spectroradiometer) sensor aboard the Terra satellite, made available by the USGS (United States Geological Survey) (https://earthexplorer.usgs.gov). NDVI data were obtained from the MOD13A2 (v006) product – Land Vegetation Indices, that provides NDVI values every 16 days period, selecting the best values in this period considering clear sky conditions and the imaging angle (Didan et al., 2015).

3. Results

3.1. Meteorological conditions

Fig. 2 shows the time series of daily global radiation data (Rg), vapor-pressure deficit (VPD), air temperature (Ta), and rainfall for the years 2014 and 2015. Rg clearly shows seasonality with higher values during the austral summer, and lower in austral winter. In 2014, Rg ranged from 11.4 MJ m^{-2} day^{-1} (07 July) to 27.6 MJ m^{-2} day^{-1} (20 January) and annual mean of 22.0 MJ m^{-2} day^{-1} (Table 1). In 2015, the same months showed minimum and maximum values of 11.0 MJ m$^{-2\ -1}$ day in 25 July and 27.5 m^{-2} MJ^{-1} day in 16 January (Fig. 2a).

The VPD ranged from 0.2 to 2.7 hPa during the year 2014 and from 0.30 to 3.0 during the year of 2015 (Fig. 2b). During 2014 the maximum and minimum values of VPD occurred in April and December, respectively. In 2015, the maximum occurred in April and the minimum in November. This behavior is expected, since April is the wettest month considering the 30-yr mean. The months of November and December mark the end of the dry season and, naturally, the driest period of the year, thus the variability of Ta (Fig. 2c) showed seasonality coherent with the seasonal cycle of Rg, which is expected in this tropical region. During 2014, the mean Ta was 28.9 °C, ranging from 24.7 °C to 32.2 °C; while in 2015, the mean was 29.5 °C, varying from 25.5 °C to 32.2 °C. The occurrence of higher Ta values during the year 2015 is attributed to the occurrence of a very strong El Niño episode, and Rg and VPD were higher than the 30-yr mean for the study area (Table 1).

Daily rainfall during 2014 and 2015 are shown in Fig. 2d. It is noted that in 2015 rainfall was more concentrated if compared to 2014. Considering rain days (days with rainfall larger than 1.0 mm), 71 were registered in 2014 while 34 were registered in 2015. Days with rainfall higher than 50 mm were observed in 2015 while such events were not observed in 2014. In almost every month of 2014 there were rainfall events, while in 2015 no rainfall event was registered from August to December. It is important to highlight that during the study period annual rainfall was considerably lower than the 30-yr mean (Table 1).

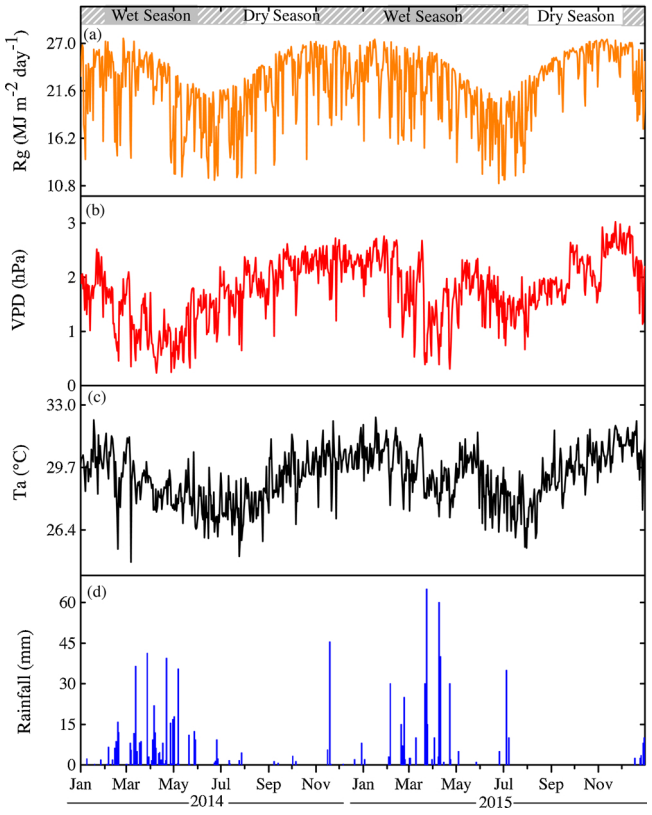

Fig. 2. Meteorological conditions during the studied period: (a) global radiation (Rg); (b) vapor-pressure deficit (VPD); (c) air temperature (Ta); (d) rainfall.

Table 1
Global radiation (Rg), air temperature (Ta), vapour pressure deficit (VPD) and rainfall annual means and climatology in the studied site.

	2014	2015	Climatology
Rg (MJ m^{-2} day^{-1})	22.0	22.6	21.6
Ta (° C)	28.9	29.5	26.8
VPD (kPa)	1.7	1.9	1.3
Rainfall (mm)	513	466	758

The annual accumulated rainfall was 513.0 and 466.6 mm, during 2014 and 2015, respectively. These values imply negative anomalies as high as 40%, since the mean climatological value is of 758.0 mm (Table 1).

These results show that weather conditions over the study area are highly affected by rainfall seasonal variability. Based on daily rainfall values, a seasonal division of the year was proposed (Fig. 2), which was used in all analysis in this study. The response of the Caatinga vegetation to rainfall is illustrated by the NDVI curve (Fig. 3), with a seasonal variability which is in accordance with the seasonal variability of rainfall during both years (Fig. 2d). During the wet season the NDVI reaches its maximum values (≈ 0.80). On the other hand, NDVI decreases consistently during the wet-dry transition season until it reaches its lowest values (≈ 0.30) in the dry season. During the dry season, leaf loss due to the desiccation tolerance mechanism in response to water stress and the increase in VPD can be interpreted as minimum NDVI values, highlighting the reduced photosynthetic activities which are restricted to the few plant species that manage to keep their leaves all year round. The maximum NDVI values in the wet season are associated with higher carbon assimilation by plants and increased vegetation productivity.

3.2. Footprint, wind direction and speed

The footprint presented seasonal variability, with values ranging from 150 m (wet season) to 200 m (dry season). However, in both cases, the footprint did not exceed the distance from the flux tower to the border of the continuous Caatinga area, which is farther than 300 m. The local wind direction during the studied period was predominantly southeast (SE) (Fig. 4).

However, a notable intensification of wind speed in 2015 (average of 2.8 m s^{-1}) relatively to 2014 (average of 2.5 m s^{-1}) was observed. Daily cycles of wind speed are shown in Fig. 5, exhibiting a bimodal pattern with similar maximums around 3.5 m s^{-1} (2015) and 3.2 m s^{-1} (2014). The first maximum occurs around 10:00 LST, associated with thermal turbulence, which is a result of the intense surface heating during the first few hours of the day, destabilizing the planetary boundary layer and intensifying wind velocity. The second maximum was observed at 21:00 LST, probably influenced by the occurrence of mechanical turbulence, by means of vertical wind shear mechanisms, which can occur intermittently during the night. In seasonal terms, the bimodal pattern was observed only during dry and dry-wet transition seasons, when the second maximum (21:00 LST) was more intense than the first one (10:00 LST). During wet and wet-dry transition seasons the second maximum was lower in magnitude in both years.

3.3. Energy partitioning

Fig. 6 shows the average daily cycle of the energy balance components observed in the Caatinga during each season in 2014 (left panel) and 2015 (right panel). Regarding mean annual values, one can note that H values corresponded to more than 50% of the Rn and that λE values corresponded to approximately 20% of Rn. In general, the components behave according to the daytime behavior of solar radiation, with maximum values occurring between 11:00 and 12:00 h (local time). Most of Rn during the daily cycle is clearly converted to H, except in the wet seasons of 2014 and 2015. However, even during the wet season, the λE portion does not exceed H, when both represent

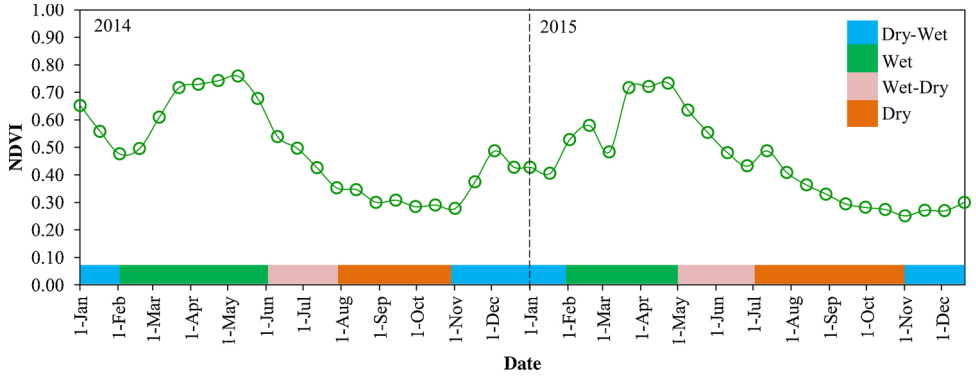

Fig. 3. NDVI in the Caatinga (ESEC-Seridó) during the years of 2014 and 2015.

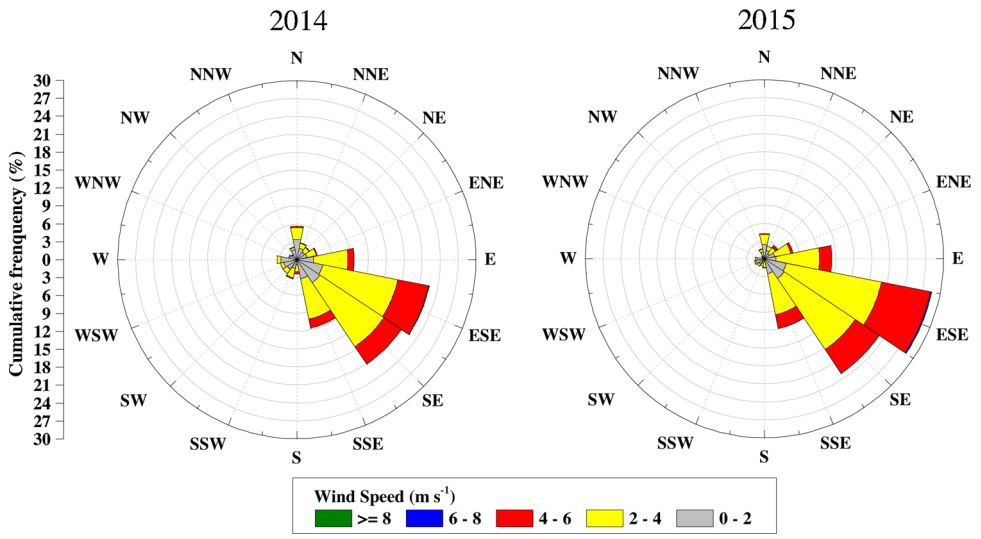

Fig. 4. Wind direction and cumulative frequency during the studied years in the study area. Colors represent wind speed classes.

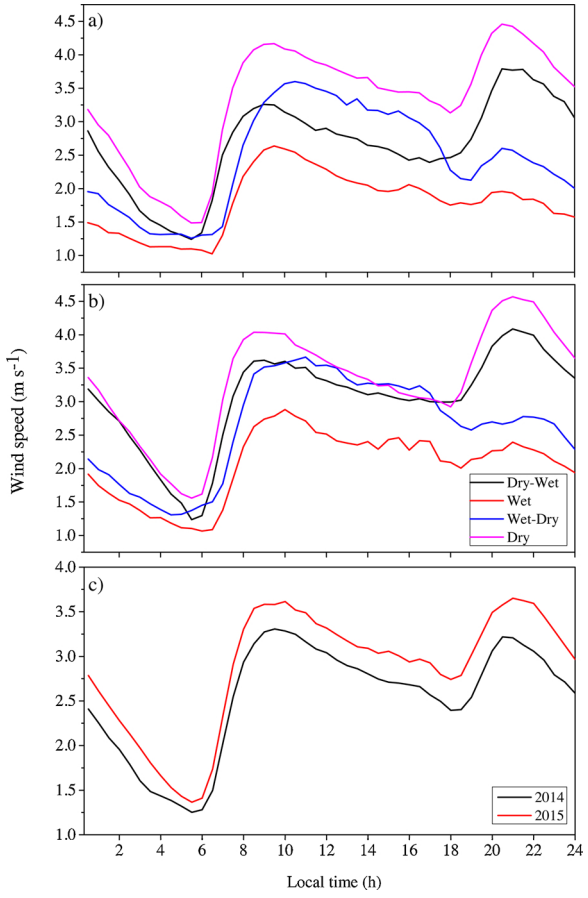

Fig. 5. Seasonal mean daily wind speed cycle during a) 2014 and b) 2015 and c) mean annual daily cycle.

around 40% of Rn. These high H values illustrate the aridity conditions to which the region has been subjected since 2012. During the dry season (Fig. 6g and h), the values of λE are very small, and during the transition seasons (Fig. 6a and b, e and f), the values of G and λE are approximately equivalent. The residual has a daytime behavior similar to that of λE in the transition seasons (Fig. 6a and b, e and f), and a quite different behavior during wet and dry seasons (Fig. 6c and d, g and h), when it is higher during the morning and decreases after 12 h (local time).

Table 2 shows the mean seasonal and annual values of the components of the energy balance and its partition, in addition to mean NDVI values. Mean seasonal Rn values ranged from 128.3 in the wet-dry season to 174.6 W m^{-2} in the dry season, in accordance with the annual variation of solar radiation. Minimum and maximum H and λE values occurred oppositely during dry and wet seasons. Mean λE fluxes ranged from 3.4 W m^{-2} (during 2014, dry season) to 71.5 W m^{-2} (during 2014, wet season), while H values ranged from 59.7 W m^{-2} (during 2014 wet-dry season) to 120.0 W m^{-2} (during the dry season of 2015). In general, mean seasonal and annual G values were low, less than 7.0 W m^{-2} and with a seasonal variability similar to that featured by H. The highest G values occurred during the dry season and during the dry-wet transition season, periods in which the Caatinga is defoliated and the soil is more exposed to radiation.

The Rn portion converted to λE during the dry season was less than 5.0%, while in the wet season it was over 40%. On the other hand, Rn portion converted to H ranged from 40% (wet season) to approximately 70% (dry season). Rn values converted into G represented less than 5% of the total Rn. The energy balance residual was 24%, ranging from 17% (wet season) to 29% (wet-dry transition) (Table 2). Still according to Table 2, one can note that the mean variability of the Bowen ratio (β) was high, ranging from 0.83 (wet season) to 35.29 (dry season), with higher values in 2015.

3.4. Energy balance closure

Energy balance closure was analyzed considering a total of 35,040 data, which 2552 (~7%) were discarded after all corrections and gap-filling were carried out. Canopy storage and photosynthesis data were not calculated. The regression coefficients between $\lambda E + H$ and $Rn - G$ for each season are shown in Table 3. The slope ranged from 0.87 (wet-dry transition season) to 0.90 (wet season) with an annual value of 0.89 in 2014 and from 0.92 (dry season) to 1.00 (wet season) with an annual value of 0.95 in 2015 (Table 3 and Fig. 7). The intercept values were all negative, ranging from -17.8 W m^{-2} (wet season) to -26.7 W m^{-2} (dry season) with an annual value of -21.9 W m^{-2} in 2014 while in 2015 the intercept ranged from -22.5 W m^{-2} (wet-dry transition season) to -31.3 W m^{-2} (dry season) with an annual value of -29.2 W m^{-2}. (Table 3 and Fig. 7). The coefficient of determination ranged from 0.95 to 0.97. EBR values varied seasonally from 0.70 (wet-dry transition season) to 0.79 (wet season) with an annual value of 0.75 in 2014 (Table 3 and Fig. 7). Still according to Table 3 and Fig.7, during 2015 the EBR varied seasonally from 0.73 (wet-dry transition season) to 0.82

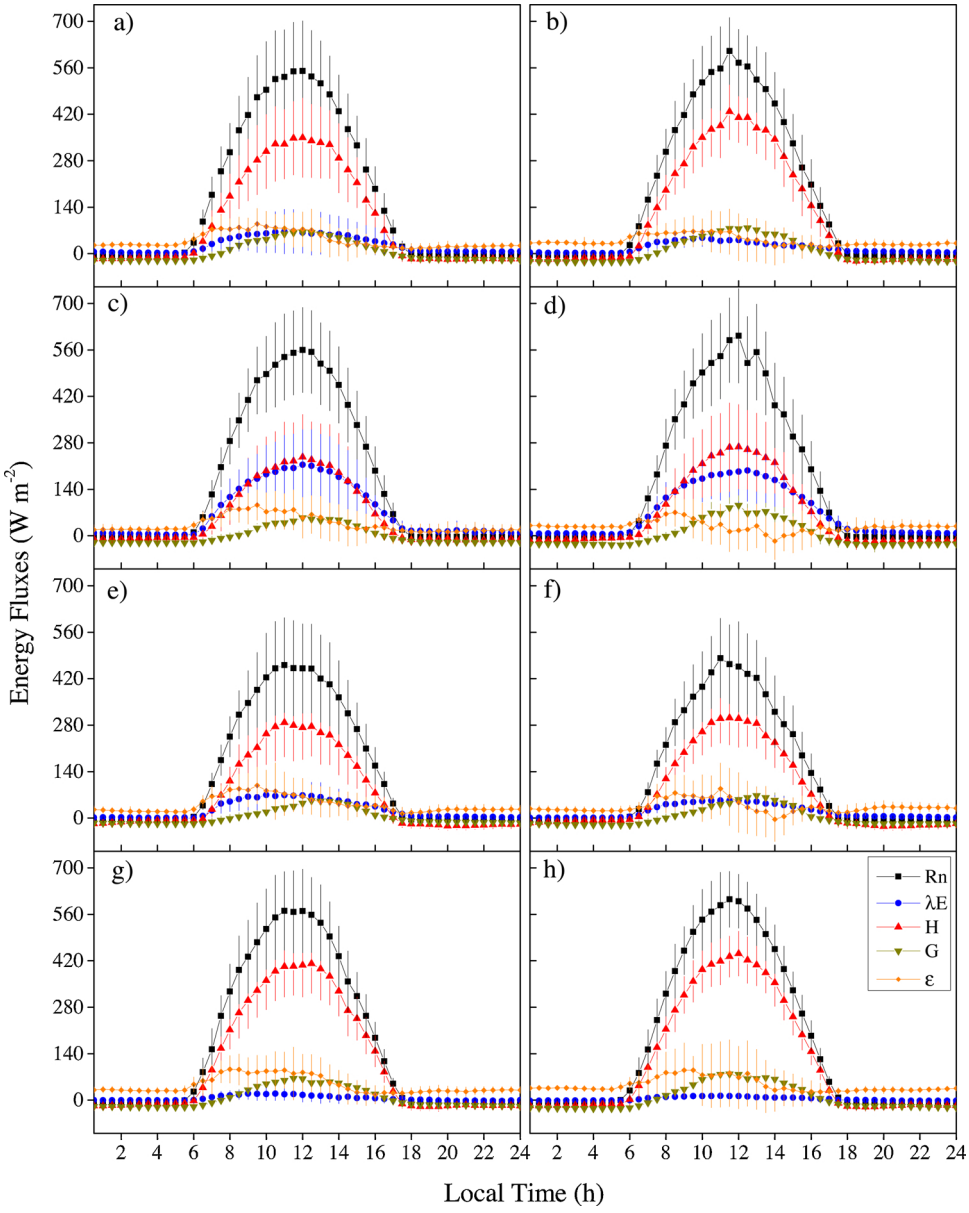

Fig. 6. Mean daily cycle of energy fluxes in 2014 (left panel) and 2015 (right panel) during dry-wet transition season (a and b); wet season (c and d); wet-dry transition season (e and f); and dry season (g and h). Vertical bars indicate the standard deviation of fluxes.

(wet season) with an annual value of 0.76, higher values during the wet season and lower values during the wet-dry transition season.

Table 3 and Fig. 7 show that during the year of 2015 energy balance closure was considerably better than in 2014. The most likely explanation for the better closure in 2015 is based on aspects of atmospheric turbulence which was more intense this year, as shown by the daily variation of friction velocity (u_*) which presents the same bimodal behavior, however with values always higher in the year 2015 (Fig. 8).

The important role of turbulence intensity in the energy balance closure is also observed through the relationship between the EBR and u_* (Fig. 9a and b). According to Fig. 9a, b and Table 4, EBR values greater than 0.70 occur for $u_* \geq 0.3$ m s^{-1} in the entire period ('All' seasons) in 2014 and for $u_* \geq 0.4$ m s^{-1} in 2015 (Table 4). On the other hand, in both years an EBR $>$ 0.70 is reached for $u_* > 0.20\, m\, s^{-1}$ in the wet season while in the dry season it is reached for $u_* > 0.40\, m\, s^{-1}$ (Table 4). During the dry-wet transition season an EBR value greater than 0.70 was found for $u_* > 0.30\, m\, s^{-1}$ in 2014 and for $u_* > 0.40\, m\, s^{-1}$ in 2015. The difference observed between both years is due to different rainfall volumes during this season. During the wet-dry transition season, EBR values greater than 0.70 were observed, in both years, for $u_* > 0.40\, m\, s^{-1}$.

In order to confirm or refuse the hypothesis that the better energy balance closure observed in 2015 if compared to 2014 was due to the higher turbulence caused by stronger winds in 2015, we calculated the annual values of the R_{wq} and R_{wT} coefficients. Fig. 10a and b show the relationship between EBR and R_{wq} and R_{wT}, respectively. The $\lambda E + H$ and $Rn - G$ data used to calculate the EBR values were grouped into 10 R_{wq} and R_{wT} categories using percentiles as described by McGloin et al. (2018). Still according to McGloin et al. (2018), because there may be relationships between R_{wq} and R_{wT} and ξ and u_* (variables which are known to influence EBC), the $\lambda E + H$ and $Rn - G$ data were limited to daytime periods when $\xi <$ -0.10 and $u_* > 0.30$ m s^{-1}. Fig. 10a shows that the relationship between EBR and R_{wq} is not direct. It is observed that for R_{wq} lower than 0.27 in 2014 and lower than 0.31 in 2015 the relationship is inverse, that is, the EBR decreases when R_{wq} increases. The relationship becomes direct for R_{wq} values higher than the aforementioned critical points (0.27 in 2014 and 0.31 in 2015). From these values on, one can clearly note that the EBR increases with the increase

Table 2
Mean values of net radiation (Rn), latent heat flux (λ E), sensible heat flux (H), soil heat flux (G), residual (ε), as well as the partitioning of the energy balance, Bowen ratio (β) and NDVI (with standard deviation) in the wet, dry and transition seasons during the studied years.

Season	Year	Rn	λE	H	G	ε	λE/Rn	H/Rn	G/Rn	ε/Rn	β	NDVI ± SD
		W m^{-2}					dimensionless					
Dry-Wet	2014	166.5	25.9	96.3	5.1	39.2	0.15	0.58	0.031	0.24	3.72	0.46 ± 0.12
	2015	172.3	17.0	111.8	5.5	38.0	0.15	0.57	0.032	0.22	6.58	0.35 ± 0.07
Wet	2014	164.6	71.5	59.7	−0.8	34.2	0.44	0.40	−0.04	0.21	0.83	0.65 ± 0.10
	2015	162.6	68.1	64.6	2.3	27.6	0.42	0.40	0.014	0.17	0.95	0.63 ± 0.10
Wet-Dry	2014	134.8	24.4	69.2	1.8	39.4	0.18	0.51	0.013	0.29	2.84	0.45 ± 0.07
	2015	128.3	19.6	73.2	1.7	33.8	0.10	0.65	0.013	0.26	3.73	0.50 ± 0.08
Dry	2014	168.7	5.2	113.7	5.4	44.4	0.03	0.67	0.032	0.26	21.87	0.31 ± 0.02
	2015	174.6	3.4	120.0	6.5	44.7	0.02	0.69	0.037	0.26	35.29	0.29 ± 0.04
All	2014	161.1	35.7	83.9	2.6	38.9	0.22	0.52	0.016	0.24	2.35	0.49 ± 0.16
	2015	159.7	25.8	93.0	4.1	36.8	0.17	0.58	0.026	0.23	3.60	0.44 ± 0.15

Table 3
Mean values of the slope, intercept and R^2 of the linear regression of λE + H against Rn-G, separated by seasons of the studied years. The values of the energy balance ratio (EBR) are also included.

Season	Dry-Wet		Wet		Wet-Dry		Dry	
	2014	2015	2014	2015	2014	2015	2014	2015
Slope	0.89	0.95	0.90	1.00	0.87	0.94	0.89	0.92
Intercept	−21,7	−29.6	−17.8	−29.2	−22.2	−25.5	−26.7	−31.3
R^2	0.97	0.97	0.95	0.95	0.96	0.95	0.97	0.97
EBR	0.75	0.77	0.79	0.82	0.70	0.73	0.75	0.75

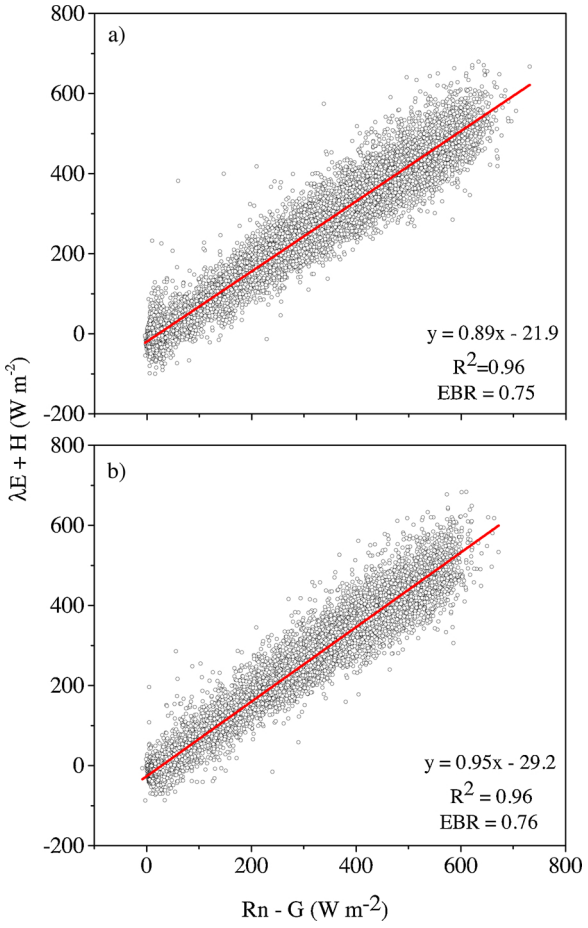

Fig. 7. Orthogonal regression between 30 min data of λE + H and Rn - G in (a) 2014 (N = 17,519) and (b) 2015 (N = 14,969). The regression results including the best fit equation and the coefficient of determination (R^2) are also shown. N is the number of samples included in the regression.

of R_{wq}. The relationship between EBR and R_{wT}, however, is direct and EBR clearly increases with increasing R_{wT} in all its ranges.

The relationship between the EBR and surface instability conditions is presented in Fig. 11a (2014) and Fig. 11b (2015), which indicate highest values of EBR (from 0.73 to 0.92) occurring under very unstable conditions ($\xi < -0.50$) to slightly unstable conditions ($-0.50 \leq \xi < -0.10$), representing approximately 50% of the data during the study period, except during the wet-dry transition and dry season in 2014 (Table 5) in which EBR values are smaller. In neutral conditions ($-10 \leq \xi \leq 10$) EBR values ranged from 0.64 (dry season of 2014) to 0.81 (wet season of 2015). On the other hand, in stable conditions ($\xi \geq 0.10$), which take place mainly during transition times (sunrise and sunset), EBR values were very low (predominantly below zero), although this condition represents less than 10% of all data during all seasons (Table 5). This behavior was observed because we

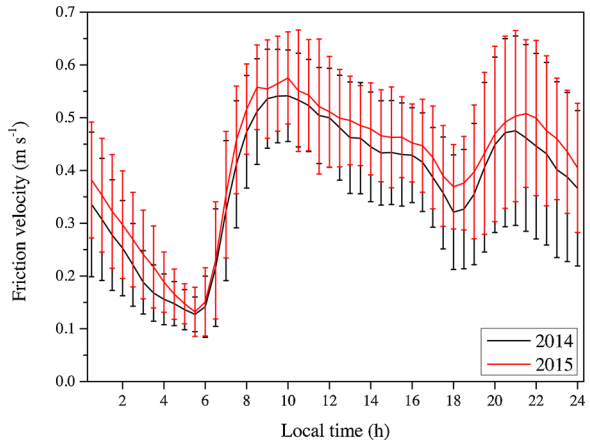

Fig. 8. Mean daily cycle of friction velocity during each studied year with standard deviation vertical bars.

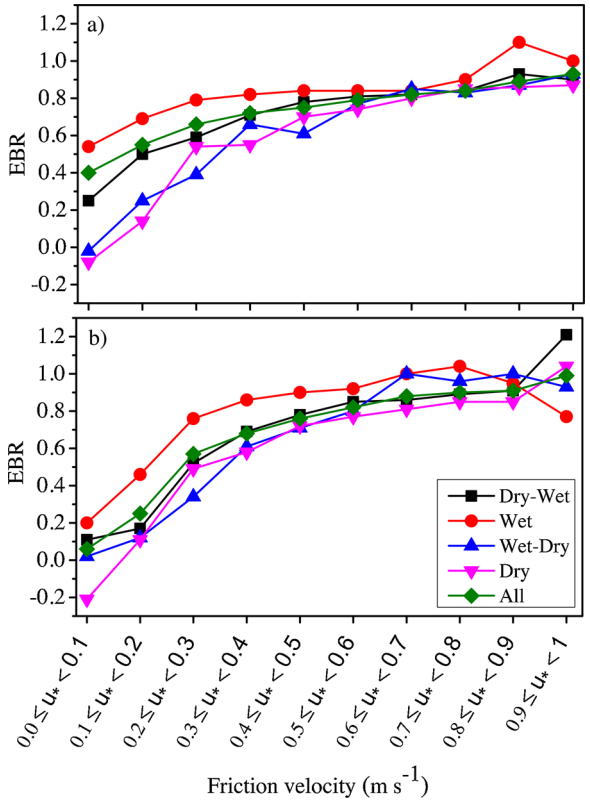

Fig. 9. The effect of u_* on the EBR during daytime in a) 2014 and b) 2105.

only took into consideration daytime data for these calculations, as carried out by Stoy et al. (2013) and McGloin et al. (2018) in previous studies.

4. Discussion

The predominant cause for the occurrence of negative rainfall anomalies which have been observed over the Brazilian semiarid region during the 2012–2016 period is the positive anomalies of sea surface temperature in the Tropical North Atlantic Ocean, favoring the northward anomalous migration of the ITCZ (Intertropical Convergence Zone) and considerably reducing the occurrence of rainfall in the region, especially in 2015 with the El Niño phenomena, as described in detail by Marengo et al. (2017a, b). Consistently, the analyzed air temperature dataset was higher if compared to climatological values, because the lack of rainfall modifies the surface radiation balance, increasing sensible heat flux and decreasing latent heat flux. Consequently, air relative humidity declined as indicated by the higher VPD (Fig. 2) and Rg reached high values, indicating less cloud cover (and consequently rainfall) for both 2014 and 2015 years (Table 1). The occurrence of minimum and maximum rainfall values during July and January (Fig. 2) is in accordance with the seasonal pattern, as result of the more prominent occurrence of convective clouds (and consequently rainfall) in the summer months as previously analyzed (Medeiros et al., 2017), while in July, cloud cover is typically stratiform, which increases top-of-atmosphere albedo and consequently decreases total Rg.

The seasonal variations in VPD are high if compared to that observed in transition forests (Vourlitis et al., 2008) or humid tropical forests (da Rocha et al., 2004), but similar to Brazilian tropical savanna (Rodrigues et al., 2014), evidencing the semi aridity of the region. The Caatinga response to rainfall seasonal variability is characterized by a marked reduction in NDVI values (Fig.3), corroborating with previous studies in the Caatinga biome (e.g., Barbosa et al., 2006; Souza et al., 2016; Silva et al., 2017), which emphasize the importance of rainfall distribution to phenology, leaf expansion and productivity in the Caatinga, as analyzed by Souza et al. (2016).

Concerning the daily cycle of wind velocity (Fig. 5), while the daytime peak can be explained by the intensification of thermal turbulence, the most probable hypothesis for the nighttime maximum is the intermittent turbulence caused by wind shear, as observed, for example, in the Amazon basin (Dias-Júnior et al., 2013; 2017). Furthermore, the seasonal variability of the nighttime maximum (Fig. 5a), can apparently be associated with low-level jets observed during the driest period (Dry-Wet and Dry seasons) along the Amazon and the Northeast Brazil (Alcântara et al., 2011).

According to Fig. 6, the daily cycle of Rn, H, and λE behaves similarly to the daily cycle of solar radiation. This behavior is expected and was also observed in other regions with different climate conditions such as the Amazon (Zeri and Sá, 2010; Gerken et al., 2018). On the other hand, it can be observed that the maximum daily G value during wet and wet-dry transition seasons occurs during the afternoon. This behavior is probably due to the occurrence of rainfall which in this region is predominantly of the convective type and associated with the ITCZ (Hastenrath, 2012), taking place mainly during the afternoon. Thus, there was an increase in soil moisture and consequently in its thermal conductivity. An increase in ε during the morning was also observed in all seasons. The same behavior was observed by Gerken et al. (2018) in a central Amazonian dry tropical forest, which was attributed to energy stored in the canopy fluxes.

The importance of rainfall seasonal variability to energy partitioning and energy balance closure in the Caatinga is evident. This importance was reported in other semiarid regions around the world (Chen et al., 2009; Majozi et al., 2017) and the results presented in Table 2 highlight it. With the establishment of the wet season, the Caatinga breaks its dormancy state, producing new leaves and thus increasing its leaf area index. During this period the Caatinga reaches the apex of its physiological and metabolic activities and the NDVI value was greater than 0.60. Thus, during said season larger portions of Rn are converted into λE (˜40%). During the dry season, the Caatinga vegetation, which consists primarily of deciduous and semi-deciduous species, reaches its minimum level of physiological and metabolic activities, which is barely sufficient for the maintenance of plants. This can be corroborated by the NDVI values which were 0.31 (2014) and 0.29 (2015) in the dry season (Table 2). During this season there is also a considerable reduction in the demand for λE and consequently most part of the Rn was converted into H (˜70%).

This seasonal variation observed in the partitioning of Rn between λE and H is highlighted by the seasonal variation of β. We observed that the driest year (2015) shows higher H values if compared to 2014, while λE fluxes were higher in 2014 (Table 2). As a consequence, during 2014 β was lower than in 2015 which can be attributed to the

Table 4
Mean energy balance ratio (EBR) values in relation to friction velocity (u*) in each season and in all seasons of the years 2014 and 2015. with the respective standard deviation and data amount (in parenthesis).

		Dry-Wet	Wet	Wet-Dry	Dry	All
$0 \leq u_* < 0.1$	2014	0.25 ± 0.35 (64)	0.54 ± 0.48 (480)	-0.02 ± 0.23 (81)	-0.08 ± 0.43 (61)	0.40 ±0.49 (686)
	2015	0.11 ± 0.35 (25)	0.20 ± 0.29 (63)	0.02 ± 0.25 (60)	-0.21 ± 0.33 (30)	0.06 ± 0.32 (178)
$0.1 \leq u_* < 0.2$	2014	0.50 ± 0.40 (130)	0.69 ± 0.33 (463)	0.25 ±0.71 (92)	0.14 ± 0.83(73)	0.55 ±0.51 (758)
	2015	0.10 ± 0.43 (47)	0.46 ± 0.44 (140)	0.12 ± 0.46 (76)	0.11 ± 0.63 (94)	0.25 ±0.52 (357)
$0.2 \leq u_* < 0.3$	2014	0.59 ± 0.71 (117)	0.79 ± 0.35 (454)	0.39 ± 1.05 (124)	0.54 ±0.57 (110)	0.66 ± 0.62 (865)
	2015	0.52 ± 0.40 (90)	0.76 ± 0.28 (208)	0.34 ± 0.77 (110)	0.49 ± 0.54 (162)	0.57 ± 0.52 (570)
$0.3 \leq u_* < 0.4$	2014	0.71 ± 0.34 (324)	0.82 ± 0.24 (565)	0.66 ± 0.43 (196)	0.55 ± 0.61 (206)	0.72 ± 0.39 (1291)
	2015	0.69 ± 0.29 (194)	0.86 ± 0.28 (275)	0.61 ± 0.59 (192)	0.58 ± 0.49 (343)	0.68 ± 0.45 (1004)
$0.4 \leq u_* < 0.5$	2014	0.78 ± 0.24 (547)	0.84 ± 0.19 (493)	0.61 ± 0.80 (311)	0.70 ± 0.43 (387)	0.75 ± 0.44 (1738)
	2015	0.78 ± 0.25 (252)	0.90 ± 0.41 (242)	0.71 ± 0.48 (284)	0.72 ± 0.36(568)	0.76 ± 0.39 (1346)
$0.5 \leq u_* < 0.6$	2014	0.81 ± 0.21 (518)	0.84 ± 0.15 (301)	0.77 ± 0.63 (327)	0.74 ± 0.40 (486)	0.79 ± 0.39 (1632)
	2015	0.85 ± 0.21 (406)	0.92 ± 0.24 (264)	0.80 ± 0.47 (344)	0.77 ± 0.34 (671)	0.82 ± 0.34 (1685)
$0.6 \leq u_* < 0.7$	2014	0.82 ± 0.21 (326)	0.84 ± 0.40 (87)	0.85 ± 0.69 (208)	0.80 ± 0.31 (482)	0.82 ± 0.40 (1113)
	2015	0.86 ± 0.18 (300)	1.00 ± 0.29 (144)	1.00 ± 2.58 (253)	0.81 ± 0.26 (596)	0.88 ± 0.45 (1293)
$0.7 \leq u_* < 0.8$	2014	0.84 ± 0.24 (103)	0.90 ± 0.36 (14)	0.83 ± 0.17 (89)	0.85 ± 0.31 (295)	0.84 ± 0.28 (501)
	2015	0.89 ± 0.15 (138)	1.04 ± 0.55 (64)	0.96 ± 0.51 (137)	0.85 ± 0.18 (294)	0.90 ± 0.33 (633)
$0.8 \leq u_* < 0.9$	2014	0.93 ± 0.77 (17)	1.30 ± 0.82 (6)	0.87 ± 0.09 (31)	0.86 ± 0.11 (81)	0.89 ± 0.34 (135)
	2015	0.91 ± 0.12 (21)	0.95 ± 0.33 (16)	1.00 ± 0.48 (47)	0.85 ± 0.17 (88)	0.91 ± 0.30 (172)
$0.9 \leq u_* \leq 1.0$	2014	0.90 ± 0.01 (2)	1.20 ± 2.20 (4)	0.93 ± 0.14 (4)	0.87 ± 0.09 (16)	0.93 ± 0.77 (26)
	2015	1.21 ± 0.51 (5)	0.77 ± 0.33 (6)	0.93 ± 0.11 (12)	1.04 ± 0.72 (16)	0.99 ± 0.54 (39)

EBR values higher than 0.80 are highlighted in gray.

fact that 2014 was a wetter year with more rain days.

The magnitude of G was around 3% of the Rn, in accordance with previous analysis over preserved areas of Caatinga (Teixeira et al., 2008; Silva et al., 2017; Pires et al., 2017). The highest G values occurred during the dry and dry-wet transition seasons (˜4% of Rn), periods in which the Caatinga has a low leaf density and the soil is more exposed to radiation. On the other hand, the two soil heat flux plates used were probably not enough to realistically represent soil cover, retrieving lower G values than expected. In order to improve these results, additional soil heat fluxes should be installed in multiple locations, as discussed by Suaer and Horton 2005 Suaer and Horton (2005).

Once again the limiting role and the importance of rainfall for the energy balance in the Caatinga is evidenced by the high seasonal variability of the energy balance residual between dry and wet seasons. The mean value of 24% of the Rn is within the range of variation commonly reported in the literature for different types of surface (Beyrich et al., 2002; Mauder et al., 2006; Franssen et al., 2010).

The degree of energy balance closure is widely used in the evaluation of the performance of EC and the quality of EC-retrieved data (Wilson et al., 2002; Baldocchi et al., 2000; Li et al., 2005). The seasonal variations of the EBR and the orthogonal regression slope are consistent, because in the wet season both arboreal vegetation and herbaceous vegetation reach a higher leaf area index and, therefore, provide greater homogeneity of soil cover, covering the usually bare soil and contributing to the better performance of eddy covariance. During said season the highest slope and EBR values were observed.

Regarding the regression between $\lambda E + H$ and $Rn - G$ (Fig. 7), the energy balance closure was of 89% in 2014 and 95% in 2015 (Fig. 7). The studied years showed slopes and intercepts comparable to those previously reported in tropical and temperate climate forests (Vourlitis et al., 2008; Giambelluca et al., 2009; del Castillo et al., 2018; Gerken et al., 2018), including the study by Wilson et al. (2002), which analyzed 22 datasets from different sites (agricultural and native biomes) of the FLUXNET network. The EBR values of 0.75 (2014) and 0.76 (2015) are also in accordance with values reported in the literature. Specifically, in semiarid savanna regions in South Africa (Majozi et al., 2017) and Central Amazon (Michiles and Gielow, 2008) the slopes found were around 0.90, while in forested area they were as high as 0.98 (Zeri and Sá, 2010). The larger slope values found in these three studies can be explained due to the incorporation of the energy storage term, which we neglected in the present study. On the other hand, if compared to previous studies in Caatinga sites (Silva et al., 2017; Pires et al., 2017), the slopes found in the present study were larger and it is worth mentioning that our data collection site is covered by preserved Caatinga.

The intercept values found in this study were all strongly negative and lower than -17 W m^{-2} (Table 3). However, there is not a well-defined pattern for the intercept found in other studies, given that this value varies between -23 and 27 W m^{-2} (Wilson et al., 2002; Michiles and Gielow, 2008; Hirando et al., 2010; Kidston et al., 2010; Majozi et al., 2017), showing relative consistency between data presented in this study and in previous studies. One possible explanation for the strong negative intercept values found in the present study is the neglected energy stored in the canopy, photosynthesis energy, soil heat

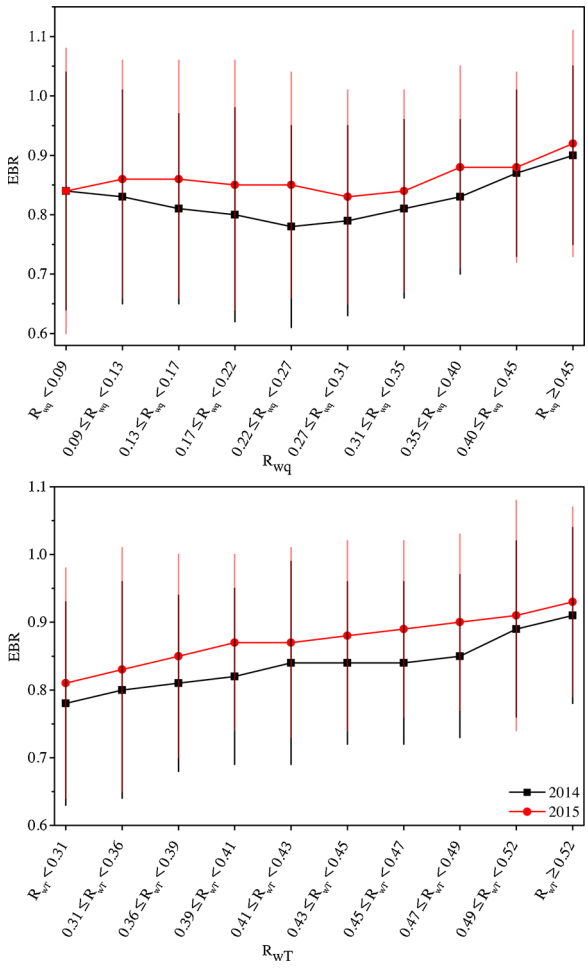

Fig. 10. The effect of a) R_{wq} and b) R_{wT} on the EBR during daytime. Vertical bars indicate the standard deviation of fluxes.

storage, among other energy balance components. Some studies have shown that incorporating these terms leads to an increase in slope values and an approximation of the intercept to zero (which is the ideal value) (Zeri and Sá, 2010; Eshonkulov et al., 2019; Kutikoff et al., 2019). Another hypothesis is due to the low Rn portion converted into G in the Caatinga during all seasons (below 3%, Table 2). It can be explained because of the low daytime duration variability which, regardless of the time of the year is around 12 h. In other words, daytime and nighttime periods have approximately the same duration during all the year. Another factor that might contribute to the improvement of the energy balance closure is the determination of heat stored in the soil above the flux plate, which wasn't calculated in the present study. Furthermore, Wilson et al. (2002) reported that soil heat flux is less impactful on the energy balance closure in forested areas than in areas with a less developed and lower canopy such as grasslands, agriculture areas and chaparral.

The seasonal values of the EBR in the Caatinga found in this study are within the range of variation for this parameter in other studies (Wilson et al., 2002; Michiles and Gielow, 2008; Li et al., 2005; Majozi et al., 2017; Stoy et al., 2013; Hirano et al., 2017). In addition, one can note that higher EBR values are identified during the wet season in the region, corroborating with the study by Michiles and Gielow (2008). These results are consistent, because in the wet season both arboreal vegetation and herbaceous vegetation reach a higher leaf area index and, therefore, provide greater homogeneity of soil cover. This greater soil homogeneity, composed by a combination of robust arboreal vegetation and herbaceous species covering the usually bare soil, contribute to the better performance of eddy covariance. It should be

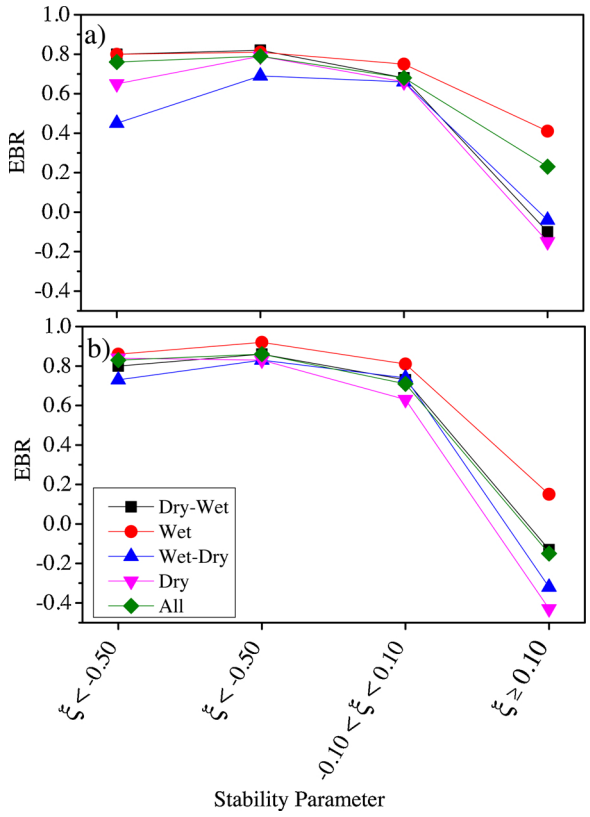

Fig. 11. The effect of ξ on the EBR during daytime in a) 2014 and b) 2015.

emphasized that a possible cause for the better closure during the wet season is the development of herbaceous vegetation in the region (Souza et al., 2012; Freitas et al., 2010; Althoff et al., 2016), which thrived only during the wet season. This result suggests a strong association between the seasonality of leaf coverage in the Caatinga and the EBR. Besides vegetation characteristics, atmospheric conditions also play a decisive role in the variations of H and λE values between the dry and wet seasons. During the dry season, H fluxes are higher, favoring the deepening of the atmospheric boundary layer (ABL) and, as consequence, intensifying local convection mechanisms (typically associated with mesoscale circulation). Contrarily, in the wet season, non-local mechanisms suppress local convection and decrease the development of the ABL, thus reducing H fluxes and partly explaining the increase in λE during this period. However, it should be noted that during the dry season non-turbulent heat fluxes also take place and are not measured by EC, which also contributes to lower λE values, as previously discussed by Gao et al. (2017) and Gerken et al. (2018).

Majozi et al. (2017) reported that in the semiarid savanna of the Kruger National Park, South Africa, moderate closure (higher imbalance) occurred during the dry season (EBR = 0.70), with the same pattern being observed in Central Amazon (Michiles and Gielow, 2008). On the other hand, the worst balance closure observed in the present study was in the wet-dry transition season, with an EBR of 0.70 in 2014 and 0.73 in 2015 (Table 3). Thus, during the wet-dry transition season the Caatinga shifts from a condition of maximum leaf cover (wet season) to the opposite condition of little or no leaf cover (dry season). During this period most arboreous species lose their leaves. In addition, all herbaceous species gradually die. Consequently, during the wet-dry transition season vegetation cover becomes extremely heterogeneous, causing the EBR to reach its lowest values. On the other hand, during the dry season, arboreous vegetation is mainly leafless and herbaceous vegetation is reduced to leaf litter (Althoff et al., 2016), forming a homogeneous and dry land cover. This allows us to infer that in the Caatinga biome both vegetation and climate dynamics play a critical

Table 5
Mean energy balance ratio (EBR) values in relation to the four classes of the stability parameter (ξ) in each season and in all seasons of the years 2014 and 2015 with the respective standard deviation and data amount (in parenthesis).

		Dry-Wet	Wet	Wet-Dry	Dry	All
$\xi < 0.5$	2014	0.80 ± 0.22 (195)	0.80 ± 0.31 (826)	0.45 ± 0.45 (82)	0.65 ± 0.40 (116)	0.76 ± 0.33 (1219)
	2015	0.80 ± 0.20 (104)	0.86 ± 0.22 (165)	0.73 ± 0.29 (78)	0.84 ± 0.20 (226)	0.83 ± 0.22 (573)
$-0.5 \leq \xi < -0.1$	2014	0.82 ± 0.16 (1092)	0.81 ± 0.21 (1079)	0.69 ± 0.32 (536)	0.79 ± 0.24 (872)	0.79 ± 0.23 (3579)
	2015	0.86 ± 0.15 (662)	0.92 ± 0.25 (642)	0.83 ± 0.20 (493)	0.83 ± 0.15 (1270)	0.86 ± 0.19 (3064)
$-0.1 < \xi < 0.1$	2014	0.68 ± 0.38 (865)	0.75 ± 0.40 (685)	0.66 ± 0.83 (776)	0.66 ± 0.54 (1188)	0.68 ± 0.56 (3514)
	2015	0.73 ± 0.33 (675)	0.81 ± 0.43 (542)	0.74 ± 1.50 (879)	0.63 ± 0.59 (1306)	0.71 ± 0.85 (3402)
$\xi \geq 0.1$	2014	−0.10 ± 1.07 (56)	0.41 ± 0.50 (275)	−0.04 ± 1.11 (69)	−0.15 ± 0.84 (31)	0.23 ± 0.78 (431)
	2015	−0.13 ± 0.24 (37)	0.15 ± 0.42 (102)	−0.32 ± 0.66 (81)	−0.43 ± 0.38 (64)	−0.15 ± 0.53 (284)

role in the energy balance closure.

The association between turbulence intensity and energy balance closure has been previously discussed in the literature (Massman and Lee, 2002; Papale et al., 2006; Moffat et al., 2007), which reported limitations during low turbulence periods, including systematic flux underestimations. Thus, better closure is expected during periods of high turbulence, according to previous studies (Barr et al., 2006; Liu et al., 2010; Sánchez et al., 2010; Stoy et al., 2013). In this way, the best fit for the energy balance was achieved with larger u_* values (Fig. 9a and Fig. 9b), corroborating with previous results obtained with data from different biomes (Wilson et al., 2002; Sánchez et al., 2010; Stoy et al., 2013; McGloin et al., 2018). In addition, negative EBR values were observed during transition seasons and the dry season (Table 4), indicating reverse fluxes during stable conditions, as observed in previous studies (e.g., Franssen et al., 2010; Stoy et al., 2013; McGloin et al., 2018).

EBR values higher than 0.80 (or higher than 80%) are typically observed in forests (Wilson et al., 2002; Foken, 2008; Stoy et al., 2013; Charuchittipan et al., 2014; Imokova et al., 2016). However, Wilson et al. (2002) found high variability in EBR values in FLUXNET sites, with variations from 0.34 to 1.60 and about 40% of the sites with EBR < 0.80. The mean EBR value determined in the present study is 0.75, which agrees with previously analyzed results.

The influence of increased vegetation cover in the Caatinga on the energy balance closure can be noted by analyzing Table 4 along with Fig. 3. During the wet season (NDVI greater than 0.70, Fig. 3), an EBR > 0.80, typical of forests according to the literature (Wilson et al., 2002; Foken, 2008; Stoy et al., 2013; Charuchittipan et al., 2014; Imokova et al., 2016) was obtained in about 60% of the data (half-hourly averages), while during the dry season (NDVI lower than 0.30, Fig. 3) said threshold was observed in about 40% of the analyzed data. We would also like to point out that, during the wet season, EBR > 0.80 was achieved when $u_* > 0.30\, m\, s^{-1}$ while in the dry season $u_* > 0.60$ was needed in order to achieve this degree of closure.

Our results indicate a strong relationship between energy balance components, NDVI and precipitation (Souza et al., 2016; Silva et al., 2017; Pires et al., 2017; Silva et al., 2017). During the culmination of plants physiological and metabolic activities, larger portions of λE were required, since the exchange of water vapor and CO_2 are intense, because deciduous plants usually have high stomatal conductance and consequently high photosynthesis and transpiration rates in favorable water availability conditions (Lambers et al., 2008). The direct effect of these factors is the reduction of λE, and Rn being mostly converted into H. This behavior is different when compared to what occurs in riparian forests and forests in the Amazon basin, where the decrease of λE values are not as pronounced because of the dense canopy which limits evaporation and the fact that those trees have deep roots, accessing deeper water reserves.

As previously discussed, the better energy balance closure in 2015 if compared to 2014 is evident. The most likely explanation for the better closure in 2015 is based on aspects of atmospheric turbulence which was more intense this year, as shown by the daily variation of wind velocity (Fig. 4 and Fig. 5) and friction velocity (u_*) (Fig. 8) which were more intense in 2015 than in 2014.

The seasonality of wind speed and direction in the Northeast Brazil is modulated mainly by large scale processes associated with the South Atlantic Subtropical High variability (Gilliland and Klein, 2018a). The interannual wind speed variability (Fig.4) is strongly influenced by ENSO phases, thus during El-Niño years (e.g., 2015) the wind speed is higher in comparison to La Niña (2014) or neutral years, as reported in previous studies (Ropelewski and Halpert, 1987; Santos and Santos e Silva, 2013; Gilliland and Klein, 2018b).

The effect of turbulence on the energy balance closure is evidenced by the direct relationship between the EBR and u_* (Fig. 9a, Fig. 9b) in which the EBR increases with the increase in u_* intensity. This relationship has been previously discussed in the literature (McGloin et al., 2018). Regarding the R_{wq} and R_{wT}.coefficients it is also evident that during 2015 they assumed higher values than in 2014. This implies that during 2014 there were larger phase differences between vertical wind velocity signals and water vapor and between vertical wind velocity signals and temperature, which are caused by large eddies (linked to entrainment and advection) (Gao et al., 2017; McGloin et al., 2018) that incurred in larger energy balance residuals in this year in comparison to 2015 during all seasons (Table 2). Fig. 10a and Fig. 10b show that the EBR increases as said coefficients also increase, especially R_{wT}. The better energy balance closure in 2015 is probably due to the more intense turbulence (more intense u_*) in 2015 combined with larger energy balance residuals observed in 2014.

The modest energy balance closure (EBR < 0.69) under very unstable and slightly unstable conditions during wet-dry transition and dry season in 2014 is probably associated with the differences between vertical wind velocity signals and water vapor and vertical wind velocity signals and temperature, as previously suggested. During said seasons the energy balance residual corresponded to more than 25% of the Rn, which were the highest values found in all the studied period. Negative EBR values were observed during transition seasons and the dry season and indicate that fluxes were reversed during stable conditions during said periods, similar to what has been reported in previous studies (Franssen et al., 2010; Stoy et al., 2013; McGloin et al., 2018).

5. Summary and conclusions

Energy balance closure and partitioning were analyzed during the years of 2014 and 2015, over a preserved fragment of the Caatinga Biome, which is a seasonally dry tropical forest in the Brazilian semiarid region. Overall, results showed that the energy balance closure in this biome was satisfactory (predominantly above 70%). The energy balance partitioning has strong seasonality, varying according to the annual distribution of rainfall. On the other hand, large scale mechanisms (ENSO phases) modulate the wind in the study area, influencing the intensity of atmospheric turbulence in such a way that during the strong El Niño year (2015) the energy balance closure was better.

The largest portion of net radiation was converted into sensible heat flux, except during the wet season, when latent heat flux assumed the

largest portions. These results show the dynamics of the Caatinga Biome is closely related to rainfall seasonality, since physiological and metabolic characteristics are modulated mainly by water available in the ecosystem.

By analyzing the energy balance closure through the orthogonal regression method an annual slope of 0.89 was found in 2014 and of 0.95 was found in 2015. The mean EBR value observed during the studied years was of 0.75. Intercept values were all negative and lower than -17.8 W m^{-2}. The probable causes for strong negative intercept values are associated with the neglecting of the air, canopy and soil heat storage terms. A better energy balance closure was observed in 2015 influenced by the more intense turbulence evidenced by higher wind and friction velocities that year. The higher wind velocity was due to 2015 being a very strong El Niño year which causes an increase in wind intensity in the tropical region. The relationship between the EBR and friction velocity was analyzed which showed that the energy balance closure is better with increasing friction velocity. Besides turbulence, the better closure in 2015 in comparison to 2014 might also be associated with the occurrence of more large eddies in 2014, which was evidenced by the R_{wq} and R_{wT} coefficients. In 2014 both coefficients were lower than those observed in 2015 which may have resulted in larger residuals that year.

Energy balance closure was also analyzed considering atmosphere instability conditions, and the best closure occurred under very unstable conditions ($\xi < -0.50$). Under stable conditions ($\xi \geq 0.10$) the closure was modest, although the amount of information analyzed under this condition was reduced. Also under stable conditions, negative EBR values were observed during transition and dry seasons, which are associated with the inversion of turbulent fluxes.

It was also observed that rainfall seasonality plays a crucial role in the energy partitioning and in the energy balance closure in the Caatinga Biome. We found that the energy balance closure presented better results during the wet season and worse results during the wet-dry transition season. During the wet season we observed that the energy balance closure is achieved during low turbulence periods. EBR values exceeding 0.80, a value commonly found in forests, were retrieved during the wet season when friction velocity values were larger than 0.30 m s^{-1}. In the dry season this threshold was achieved only when the friction velocity was equal to or greater than 0.60 m s^{-1}.

It is important to highlight that the two studied years were of extreme drought and, consequently, with shorter than usual wet seasons (Marengo et al., 2017a, b). Therefore, it is expected that during years of heavy rains, the wet season should last longer and the energy balance closure should be more efficient.

Acknowledgments

The authors are thankful to the Brazilian National Institute of the Semiarid (INSA) for providing the eddy covariance data used in this study which is partially based on the Thesis by Suany Campos carried out in the Climate Sciences Post-graduate Program of the Federal University of Rio Grande do Norte. The authors are also thankful to the Coordination for the Improvement of Higher Education Personnel (CAPES) for the scholarship granted to the first author (Process nº 1441772); to the National Council for Scientific and Technological Development (CNPq) for funding the NOWCDCB network research project (nº 465764/2014-2 and 446172/2015-4) and for the research productivity grant seventh, eleventh, and thirteenth authors (Processes nº 301348/2015-4, 309165/2010-5, and 303061/2014-6, respectively); to the ICMBio (Chico Mendes Institute for Biodiversity Conservation) for providing the experimental area and to the ESEC-Seridó (Ecological Station of Seridó) for supporting experimental activities. The author are also thankful to The University of Edinburgh for providing the Edire (http://www.geos.ed.ac.uk/abs/research/micromet/EdiRe/) software and to the Max Planck Institute for Biogeochemistry for the online tool used for gap filling (http://www.bgc-jena.mpg.de/~MDIwork/eddyproc/). The authors would also like to honor Dr. Ignacio Hernán Salcedo (*in memorian*), Emeritus Professor at the Federal University of Pernambuco, former President of the INSA (2011-2015) and one of the creators of the NOWCDCB network.

References

Alcântara, C.R., Silva Dias, M.A.F., Souza, E.P., Cohen, J.C.P., 2011. Verification of the role of the low level jets in Amazon squall lines. Atmos. Res. 100, 36–44. https://doi.org/10.1016/j.atmosres.2010.12.023.

Allen, R.G., Pereira, L.S., Raes, D., Smith, M., 1998. Crop evapotranspiration: guidelines for computing crop water requirements. United Nations FAO, Irrigation and Drainage Paper 56. FAO, Rome, Italy.

Allen, K., Dupuy, J.M., Gei, M.G., Hulsof, C., Medvigy, D., Pizano, C., Salty-Negret, B., Smith, C.M., Trierweiler, A., van Bloem, S.J., Waring, B.G., Xu, X., Powers, J.S., 2017. Seasonally dry tropical forests will be sensitive or resistant to future changes in rainfall regimes? Environ. Res. Lett. 12, 023001. https://doi.org/10.1088/1748-9326/aa5968.

Althoff, T.D., Menezes, R.S.C., Carvalho, A.L., Pinto, A.S., Santiago, G.A.C.F., Ometto, J.P.H.B., von Randow, C., Sampaio, E.V.S.B., 2016. Climate change impacts on the sustainability of the firewood harvest and vegetation and soil carbon stocks in a tropical forest in Santa Tersinha Municipality, Northeast Brazil. For. Ecol. Manag. 360, 367–375. https://doi.org/10.1016/j.foreco.2015.10.001.

Alvares, C.A., Stape, J.L., Sentelhas, P.C., Gonçalves, J.L.M., Sparovek, G., 2014. Köppen's climate classification map for Brazil. Meteorol. Z. 22 (6), 711–728. https://doi.org/10.1127/0941-2948/2013/0507.

Araújo, A.C., Dolman, A.J., Waterloo, M.J., Gash, J.H.C., Kruijt, B., Zanchi, F.B., de Lange, J.M.E., Stoevelaar, R., Manzi, A.O., Nobre, C.A., Lootens, R.N., Becker, J., 2010. The spatial variability of CO_2 storage and the interpretation of eddy covariance fluxes in central Amazonia. Agric. For. Meteorol. 150, 226–237. https://doi.org/10.1016/j.agrformet.2009.11.005.

Baldocchi, D., 2008. "Breathing" of the terrestrial biosphere: lessons learned from a global network of carbon dioxide flux measurement systems. Aust. J. Bot. 56, 1–26. https://doi.org/10.1071/BT07151.

Baldocchi, D.D., Law, B.E., Anthoni, P.M., 2000. On measuring and modeling energy fluxes above the floor of a homogeneous and heterogeneous conifer forest Agric. Forest Meteorol. 102, 187–206. https://doi.org/10.1016/s0168-1923(00)00098-8.

Baldocchi, D., Falge, E., Gu, L.H., Olson, R., Hollinger, D., Running, S., Anthoni, P., Bernhofer, C., Davis, K., Evans, R., Fuentes, J., Goldstein, A., Katul, G., Law, B., Lee, X.H., Malhi, Y., Meyers, T., Munger, W., Oechel, W., Paw U, K.T., Pilegaard, K., Schmid, H.P., Valentini, R., Verma, S., Vesala, T., Wilson, K., Wofsy, S., 2001. FLUXNET: a new tool to study the temporal and spatial variability of ecosystem-scale carbon dioxide, water vapor, and energy flux densities. Bull. Am. Meteorol. Soc. 82, 2415–2434. https://doi.org/10.1175/1520-0477(2001)082<2415:FANTTS>2.3.CO;2.

Baldocchi, D., Xu, L., Kiang, N., 2004. How plant functional-type, weather, seasonal drought, and soil physical properties alter and energy fluxes of an oak-grass savanna and an annual grassland. Agric. For. Meteorol. 123, 13–39. https://doi.org/10.1016/j.agrformet.2003.11.006.

Banda-R, K., Delgado-Salinas, A., Dexter, K.G., Linares-Palomino, R., Oliveira-Fiho, A., Prado, D., Pullan, M., Quitana, C., Riina, R., Rodríguez, G.M., Weintritt, J., Acebedo-Rodríguez, P., Adarve, J., Álvarez, E., Aranguren B, A., Artega, J.C., Aymard, G., Castaño, A., Ceballos-Mago, Á., Cogollo, Á., Cuadros, H., Delgado, F., Devia, W., Dueñas, H., Fajardo, L., Fern´nadez, à., Fernández, M.Á., Franklin, J., Freid, E.H., Galetti, L.A., Gonto, R., González-M, R., Graveson, R., Helmer, E.H., Idárraga, Á., López, R., Marcano-Vega, H., Martínez, O.G., Maturo, H.M., McDonald, M., McLaren, K., Melo, O., Mijares, F., Mogni, V., Molina, D., Moreno, N.P., Nassar, J.M., Neves, D.M., Oakley, L.J., Oatham, M., Olvera-Luna, A.R., Pezzini, F.F., Dominguez, O.J.R., Ríos, M.E., Rivera, O., Rodríguez, N., Rojas, A., Särkinen, Sánchez, R., Smith, M., Vargas, C., Villanueva, B., Pennington, R.T., 2016. Plant diversity patterns in neotropical dry tropical forests and their conservation implications. Science. 353, 1383–1387. https://doi.org/10.1126/science.aaf5080.

Barbosa, H.A., Huete, A.R., Baethgen, W.E., 2006. A 20-year study of NDVI variability over the Northeast Region of Brazil. J. Arid Environ. 67, 288–307. https://doi.org/10.1016/j.jaridenv.2006.02.022.

Barr, A.G., Morgenstern, K., Black, T.A., McCaughey, J.H., Nesic, Z., 2006. Surface energy balance closure by the eddy-covariance method above three boreal forest stands and implications for the measurements of the CO_2 flux. Agric. For. Meteorol. 140, 322–337. https://doi.org/10.1016/j.agrformet.2006.08.007.

Beyrich, F., Richter, S.H., Weisensee, U., Kohsiek, W., Lohse, H., De Bruin, H.A.R., Foken, T., Göckede, M., Berger, F., Vogt, R., Batchvarova, E., 2002. Experimental determination of turbulent fluxes over the heterogeneous LITFASS area: selected results from the LITFASS-98 experiment. Theor. Appl. Climatol. 73, 19–34. https://doi.org/10.1007/s00704-002-0691-7.

Biudes, M.S., Vourlitis, G.L., Machado, N.G., Arruda, P.H.Z., Neves, G.A.R., Lobo, F.A., Neale, C.M.U., Nogueira, J.S., 2015. Patterns of energy balance exchange for tropical ecosystems across a climate gradient in Mato Grosso, Brazil. Agric. For. Meterol. 202, 112–124. https://doi.org/10.1016/j.agrformet.2014.12.008.

Cabral, O.M.R., Rocha, H.R., Gash, J.H.C., Ligo, M.A.V., Freitas, H.C., Tatsch, J.D., 2010. The energy and water balance of a *Eucalyptus* plantation in southeast Brazil. J. Hydrol. 388, 208–216. https://doi.org/10.1016/j.jhydrol.2010.04.041.

Cabral, O.M.R., Rocha, H.R., Gash, J.H., Freitas, H.C., Ligo, M.A.V., 2015. Water and

energy fluxes from woodland savanna (cerrado) in southeast Brazil. J. Hydrol.: Reg. Stud. 4, 22–40. https://doi.org/10.1016/j.ejrh.2015.04.010.
Campbell Scientific Inc, 2012. EC150 CO_2 And H_2O Open-path Gas Analyzer and EC100 Electronics With Optional CSAT3A 3D Sonic Anemometer. User Manual.ftp://ftp.campbellsci.com/pub/csl/outgoing/uk/manuals/ec150.pdf(Accessed 15, November 2018). .
Charuchittipan, D., Babel, W., Mauder, M., Leps, J.-P., Foken, T., 2014. Extension of the averaging time in eddy-covariance measurements and its effect on the energy balance closure. Bound-Layer Meteorol. 152, 303–327. https://doi.org/10.1007/s10546-014-9922-6.
Chen, S., Chen, J., Lin, G., Zhang, W., Miao, H., Wei, L., Huang, J., Han, X., 2009. Energy balance and partition in Inner Mongolia steppe ecosystems with different land use types. Agric. For. Meteorol. 149, 1800–1809. https://doi.org/10.1016/j.agrformet.2009.06.009.
da Rocha, H.R., Goulden, M.L., Miller, S.D., Menton, M.C., Pinto, L.D.V.O., Freitas, H.C., Silva Figueira, A.M., 2004. Seasonality of water and heat fluxes over a tropical forest in eastern Amazonia. Ecol. Appl. 14, 522–532. https://doi.org/10.1890/02-6001.
da Rocha, H.R., Manzi, A.O., Cabral, O.M., Miller, S.D., Goulden, M.L., Saleska, S.R., -Coupe, N.R., Wosfy, S.C., Borma, L.S., Artaxo, P., Vourlistis, G., Nogueira, J.S., Cardoso, F.L., Nobre, A.D., Kruijt, B., Freitas, H.C., von Randow, C., Aguiar, R.G., Maia, J.F., 2009. Patterns of water and heat flux across a biome gradient from tropical forest to savanna in Brazil. J. Geophys. Res. 114, G0012. https://doi.org/10.1029/2007JG000640.
del Castillo, E.G., Paw U, K.T., Sánchez-Azofeifa, A., 2018. Turbulence scales for eddy covariance quality control over a tropical dry forest in complex terrain. Agric. For. Meteorol. 249, 390–406. https://doi.org/10.1016/j.agrformet.2017.11.014.
Dias-Júnior, Q.C., Sá, L.D.A., Pachêco, V.B., Souza, C.M., 2013. Coherent structures detected in the unstable atmospheric surface layer above the Amazon forest. J. Wind Eng. Ind. Aerodyn. 115, 1–8. https://doi.org/10.1016/j.jweia.2012.12.019.
Dias-Junior, C.Q., Sá, L.D.A., Marques Filho, E.P., Santana, R.A., Mauder, M., Manzi, A.O., 2017. Turbulence regimes in the stable boundary layer above and within the Amazon forest. Agric. For. Meteorol. 233, 122–132. https://doi.org/10.1016/j.agrformet.2016.11.001.
Didan, K., Munoz, A.B., Solana, R., Huete, A., 2015. MODIS Vegetation Index User's Guide (MOD13 Series). The University of Arizona, Tucson. Available in:http://vip.arizona.eduAccess in 2018 May.
Dombroski, J.L.D., Prazedes, S.C., Freitas, R.M.O., Pontes, F.M., 2011. Water relations of Caatinga trees in the dry season. S. Afr. J. Bot. 77, 430–434. https://doi.org/10.1016/j.sajb.2010.11.001.
Eder, F., De Roo, F., Kohnert, K., Desjardins, R.L., Schimid, H.P., Mauder, M., 2014. Evaluation of two energy balance closure parametrizations. Boud.-Layer Meteorol. 151, 195–219. https://doi.org/10.1007/s10546-013-9904-0.
EMBRAPA, 2006. Sistema Brasileiro De Classificação De Solos, 2.ed. EMBRAPA-Solos, Rio de Janeiro.
Eshonkulov, R., Poyda, A., Ingwersen, J., Pulatov, A., Streck, T., 2019. Improving the energy balance closure over a winter wheat field by account for minor storage terms. Agric. For. Meteorol. 264, 283. https://doi.org/10.1016/j.agrformet.2018.10.012.
Foken, T., 2008. The energy balance closure problem: an overview. Ecol. Appl. 18 (6). https://doi.org/10.1890/06-0922.1. 1351-167.
Foley, J.A., Costa, M.H., Delire, C., Ramankutty, N., Snyder, P., 2003. Green surprise? How terrestrial ecosystems could affect earth's climate. Front. Ecol. Environ. 1 (1), 38–44. https://doi.org/10.1890/1540-9295(2003)001[0038:GSHTEC]2.0.CO;2.
Franssen, H.J.H., Stöckli, R., Lehner, I., Rotenberg, E., Seneviratne, S.I., 2010. Energy balance closure of eddy-covariance data: a multisite analysis for European FLUXNET stations. Agric. For. Meteorol. 150, 1553–1567. https://doi.org/10.1016/j.agrformet.2010.08.005.
Freitas, A.D.S., Sampaio, E.V.S.B., Fernandes, A.R., Santos, C.E.R.S., 2010. Biological nitrogen fixation in legume trees of the Brazilian caatinga. J. Arid Environ. 74, 344–349. https://doi.org/10.1016/j.jaridenv.2009.09.018.
Gao, Z., Liu, H., Katul, G.G., Foken, T., 2017. Non-closure of the surface energy balance explained by phase difference between vertical velocity and scalars of large atmospheric eddies. Environ. Res. Lett. 12 (3). https://doi.org/10.1088/1748-9326/aa625b. 034025.
Georg, W., Albin, H., Georg, N., Katharina, S., Enrico, T., Peng, Z., 2016. On the energy balance closure and net radiation in complex terrain. Agric. For. Meteorol. 226-227, 37–49. https://doi.org/10.1016/j.agrformet.2016.05.012.
Gerken, T., Ruddell, B.L., Fuentes, J.D., Araújo, A., Brunsell, N.A., Maia, J., Manzi, A., Mercer, J., Santos, R.N., von Randow, C., Stoy, P.C., 2018. Investigating the mechanisms responsible for the lack of surface energy balance closure in a central Amazonian tropical rainforest. Agric. For. Meteorol. 255, 92–103. https://doi.org/10.1016/j.agrformet.2017.03.023.
Giambelluca, T.W., Scholz, F.G., Bucci, S.J., Meinzer, F.C., Goldstein, G., Hoffmann, W.A., Franco, A.C., Buchert, M.P., 2009. Evapotranspiration and energy balance of Brazilians savannas with contrasting tree density. Agric. For. Meteorol. 149, 1365–1376. https://doi.org/10.1016/j.agrformet.2009.03.006.
Gilliland, J.M., Klein, B.D., 2018a. Position of the South Atlantic anticyclone and its impact on surface conditions across Brazil. J. Appl. Meteorol. Climatol. 57 (3), 535–553. https://doi.org/10.1175/JAMC-D-17-0178.1.
Gilliland, J.M., Klein, B.D., 2018b. Surface wind speed: trend and climatology of Brazil from 1980-2014. Int. J. Climatol. 38 (2), 1060–1073. https://doi.org/10.1002/joc.5237.
Gu, L., Massman, W.J., Leuning, R., Pallardy, S.G., Meyers, T., Hanson, P.J., Riggs, J.S., Hosman, K.P., Yang, B., 2012. The fundamental equation of eddy covariance and its application in flux measurements. Agric. For. Meteorol. 152, 135–148. https://doi.org/10.1016/j.agrormet.2011.09.014.
Hao, Y., Wang, Y., Huang, X., Cui, X., Zhou, X., Wang, S., Niu, H., Jiang, G., 2007. Season and interannual variation in water vapor and energy exchange over a typical steppe in Inner Mongolia. China. Agric. For. Meteorol. 146, 57–69. https://doi.org/10.1016/j.agrformet.2007.05.005.
Hastenrath, S., 2012. Exploring the climate problems of Brazil's Nordeste: a review. Clim. Change 112 (2), 243–251. https://doi.org/10.1007/s10584-011-0227-1.
Heilman, J.L., McInnes, K.J., Savage, M.J., Gesch, R.W., Lascano, R.J., 1994. Soil and canopy energy balances in a west Texas vineyard. Agric. For, Meteorol. 71, 99–114. https://doi.org/10.1016/0168-1923(94)90102-3.
Hirano, T., Suzuki, K., Hirata, R., 2017. Energy balance and evapotranspiration changes in a larch forest caused by severe disturbance an early secondary succession. Agric. For. Meteorol. 232, 457–468. https://doi.org/10.1016/j.agrformet.2016.10.003.
Holzman, B.A., 2008. Tropical Forest Biomes. Greenwood Press, Westport.
Imokova, K., Ingwersen, J., Hevart, M., Streck, T., 2016. Energy balance closure on a winter wheat stand: comparing the eddy covariance technique with the soil water balance method. Biogeosci. 13, 63–75. https://doi.org/10.5194/bg-13-63-2016.
INMET, 1992. Normais Climatológicas. INMET, Brasília, pp. 1961–1990.
Jaeger, E.B., Stöckli, R., Seneviratne, S.I., 2009. Analysis of planetary boundary layer fluxes and land–atmosphere coupling in the regional climate model CLM. J. Geophys. Res. 114, D17106. https://doi.org/10.1029/2008JD011658.
Kaimal, J.C., Finnigan, J.J., 1994. Atmospheric Boundary Layer Flows: Their Structure and Measurement. Oxford University Press, New York, USA.
Kidston, J., Brümmer, C., Black, T.A., Morgenstern, K., Nesic, Z., McCaughey, J.H., Barr, A.G., 2010. Energy balance closure using eddy covariance above two different land surfaces and implications for CO2 flux measurements. Boundary-Layer Meteorol. 136, 193–218. https://doi.org/10.1007/s10546-010-9507-y.
Kljun, N., Calanca, P., Rotach, M., Schmid, H., 2015. A simple two-dimensional parameterisation for Flux Footprint Prediction (FFP). Geosci. Model Dev. 8 (11), 3695–3713. https://doi.org/10.5194/gmd-8-3695-2015.
Koch, R., Almeida-Cortez, J.S., Kleinschmit, B., 2017. Revealing areas of high nature conservation importance in a seasonally dry tropical forest in Brazil: combination of modelled plant diversity hot spots and threat patterns. J. Nat. Conserv. 35, 24–39. https://doi.org/10.1016/j.jnc.2016.11.004.
Kutikoff, S., Lin, X., Evett, S., Gowda, P., Moorhead, J., Marek, G., Colaizzi, P., Aiken, R., Brauer, D., 2019. Heat storage and its effect on the surface energy balance closure under advective conditions. Agric. For. Meteorol. 265, 56–69. https://doi.org/10.1016/j.agrformet.2018.10.018.
Lambers, H., Capin III, F.S., Pons, T.L., 2008. Plant Physiologicl Ecology, second ed. Springer, New York.
Leuning, R., van Gorsel, E., Massman, W.J., Isaac, P.R., 2012. Reflections on the surface energy imbalance problem. Agric. For. Meteorol. 156, 65–74. https://doi.org/10.1016/j.agrformet.2011.12.002.
Li, Z.Q., Yu, G.R., Wen, X.F., Zhang, L.M., Ren, C.Y., Fu, Y.L., 2005. Energy balance closure at ChinaFLUX sites. Sci. China Ser. D-Earth Sci. 48, 51–62. https://doi.org/10.1360/05zd0005.
Linares-Palomino, R., Oliveira-Filho, A.T., Pennington, R.T., 2011. Neotropical seasonally dry forests: diversity, endemism and biogeography of woody plants. In: Dirzo, R., Young, H.S., Mooney, H.A., Ceballos, G. (Eds.), Seasonally Dry Tropical Forests: Ecology and Conservation. Island Press, Washington, pp. 3–21.
Luyssaert, S., Inglima, I., Jungs, M., Richardson, A.D., Reichstein, M., Papale, D., Piao, S.L., Shulzes, E.D., Wingate, L., Matteucci, G., Aragão, L., Aubinet, M., Beer, C., Bernhofer, C., Black, K.G., Bonal, D., Bonnefond, M., Chambers, J., Ciais, P., Cook, B., Davis, K.J., Dolman, A.J., Gielen, B., Goulden, M., Grace, J., Granier, A., Grele, A., Griffis, T., Grünwald, T., Guidolotti, G., Hanson, P.J., Harding, R., Hollinger, D.Y., Hutyra, L.R., Kolari, P., Kruijt, B., Kutsh, W., Lagergren, F., Laurila, T., Law, B.E., Le Maire, G., Lindroth, A., Loustau, D., Malhi, Y., Mateus, J., Migliavacca, M., Misson, L., Montagnani, L., Moncrieff, J., Moors, E., Munger, J.W., Nikinmaa, E., Ollinger, S.V., Pita, G., Rebmann, C., Roupsard, O., Saigusa, N., Sanz, M.J., Seufert, G., Sierra, C., Smith, M.L., Tang, J., Valentini, R., Vesala, T., Jansses, I.A., 2007. CO_2 balance of boreal, temperate, and tropical forest derived from a global database. Glob. Change Biol. 13, 2509–2537. https://doi.org/10.1111/j.1365-2486.2007.01439.x.
Majozi, N.P., Mannaerts, C.M., Ramoelo, A., Mathieu, R., Nickless, A., Verhoef, W., 2017. Analysing surface energy balance closure and partitioning over a semi-arid savanna FLUXNET site in Skukuza, Kruger National Park, South Africa. Hydrol. Earth Syst. Sci. 21, 3401–3415. https://doi.org/10.5194/hess-21-3401-2017.
Marengo, J.A., Bernasconi, M., 2015. Regional differences in aridity/drought conditions over Northeast Brazil: present state and future projections. Clim. Chang. 129, 103–115. https://doi.org/10.1007/s10584-014-1310-1.
Marengo, J.A., Alves, L.M., Alvalá, R.C.S., Cunha, A.P., Brito, S., Moraes, O.L.L., 2017a. Climatic characteristics of the 2010-2016 drought in the semiarid Northeast Brazil region. Ann. Braz. Acad. Sci. https://doi.org/10.1590/0001-3765201720170206.
Marengo, J.A., Torres, R.R., Alves, L.M., 2017b. Drought in Northeast-Brazil - past, present, and future. Theor. Appl. Climatol. 129, 1189–1200. https://doi.org/10.1007/s00704.016-1840-8.
Massman, W.J., 2000. A simple method for estimating frequency response corrections for eddy covariance systems. Agric. For. Meteorol. 104, 185–198. https://doi.org/10.1016/S0168-1923(00)00164-7.
Massman, W.J., Lee, X., 2002. Eddy covariance flux corrections and uncertainties in long-term studies of carbon and energy exchanges. Agric. For. Meteorol. 113, 121–144. https://doi.org/10.1016/S0168-1923(02)00105-3.
Mauder, M., Foken, T., 2004. Documentation and Instruction Manual of the Eddy Covariance Software Package TK2. University of Bayreuth, Bayreuth.
McGloin, R., Šigut, L., Havránková, K., Dušek, J., Pavelka, M., Sedlák, P., 2018. Energy balance closure at a variety of ecosystems in Central Europe with contrasting topographies. Agric. For. Meteorol. 248, 418–431. https://doi.org/10.1016/j.agrformet.2017.10.003.
Medeiros, F.J., Santos e Silva, C.M., Bezerra, B.G., 2017. Calibration of ångström-prescott

equation to estimate daily solar radiation on Rio Grande do norte state, Brazil. Rev. Bras. Meteorol. 32, 409–416. https://doi.org/10.1590/0102-77863230008.
Meir, P., Metcalfe, D.B., Costa, A.C.L., Fisher, R.A., 2008. The fate of assimilated carbon during drought: impacts on respiration in Amazon rainforests. Philos. Trans. R. Soc. B. 363, 1849–1855. https://doi.org/10.1098/rstb.2007.0021.
Michiles, A.A.S., Gielow, R., 2008. Above-ground thermal energy storage rates, trunk heat fluxes and surface energy balance in a central Amazonian rainforest. Agric. For. Meteorol. 148, 917–930. https://doi.org/10.1016/j.agrformet.2008.01.001.
Mittermeier, R.A., Mittermeier, C.G., Brooks, T.M., Konstantin, W.R., Fonseca, G.A.B., Kormos, C., 2003. Wilderness and biodiversity conservation. Proc. Natl Acad. Sci. 100 (18), 10309–10313. https://doi.org/10.1073/pnas.1732458100.
Moffat, A.M., Papale, D., Reichstein, M., Hollinger, D.Y., Richardson, A.D., Barr, A.G., Beckstein, C., Braswell, B.H., Churkina, G., Desai, A.R., Falge, E., Gove, J.H., Heimann, M., Hui, D., Jarvis, A.J., Kattge, J., Noormets, A., Stauch, V.J., 2007. Comprehensive comparison of gap-filling techniques for eddy covariance net carbono fluxes. Agric. For. Meteorol. 147, 209–232. https://doi.org/10.1016/j.agrformet.2007.08.011.
Moncrieff, J., Clement, R., Finnigan, J., Meyers, T., 2005. Averaging, detrending, and filtering of eddy covariance time series. In: Lee, X., Massman, W., Law, B.E. (Eds.), Handbook of Micrometeorology. Springer, Berlim, pp. 7–31.
Moore, C.J., 1986. Frequency response corrections for eddy correlation systems. Boud.-Layer Meteorol. 37, 17–35.
Murphy, P., Lugo, A., 1986. Ecology of tropical dry forest. Annu. Rev. 17, 67–88.
Oliveira, P.T., Santos e Silva, C.M., Lima, K.C., 2017. Climatology and trend analysis of extreme precipitation in subregions of Northeast Brazil. Theor. Appl. Climatol. 130, 77–90 https://doi-org.ez18.periodicos.capes.gov.br/10.1007/s00704-016-1865-z.
Pagoto, M.A., Roig, F.A., Ribeiro, A.S., Lisi, C.S., 2015. Influence of regional rainfall and Atlantic sea surface temperature on tree-ring growth of *Poincianella pyramidalis*, semiarid forest from Brazil. Dendrochronologia 35, 14–23. https://doi.org/10.1016/j.dendro.2015.05.007.
Papale, D., Reichstein, M., Aubinet, M., Canfora, E., Bernhofer, C., Kutsch, W., Longdoz, B., Rambal, S., Valentini, R., Vesala, T., Yakir, D., 2006. Towards a standardized processing of Net Ecosystem Exchange measured with eddy covariance technique: algorithms and uncertainty estimation. Biogeoscience 3, 571–583. https://doi.org/10.5194/bg-3-571-2006.
PBMC, 2014. In: Ambrizzi, T., Ahmad, M. (Eds.), Scientific Basis of Climate Change. Contribution of Working Group 1 of the Brazilian Climate Change Panel to the First National Assessment Report on Climate Change. COPPE, Federal University of Rio de Janeiro, Rio de Janeiro.
Pennington, R.T., Lewis, G.P., Ratter, J.A., 2006. An overview of the plant diversity, biogeography, and conservation of neotropical savannas and seasonally dry forests. In: Pennington, R.T., Lewis, G.P., Ratter, J.A. (Eds.), Neotropical Savannas and Seasonally Dry Forests: Diversities, Biogeography, and Conservation. Taylor & Francis Group, Boca Raton, pp. 1–29.
Pielke, R.A., Avissar, R., Raupach, M., Dolman, A.J., Zeng, X., Denning, A.S., 1998. Interactions between the atmosphere and terrestrial ecosystems: influence on weather and climate. Glob. Chang. Biol. 4, 461–475. https://doi.org/10.1046/j.1365-2486.1998.t01-1-00176.x.
Pires, W.N., Moura, M.S.B., Souza, L.S.B., Silva, T.G.F., Carvalho, H.F.S., 2017. Fluxos de radiação, energia, CO_2 e vapor de água em uma área de caatinga em regeneração. Agrometoeros. 25 (1), 143–151 (In Portuguese).
Reichstein, M., Falge, E., Baldocchi, D., Papale, D., Aubinet, M., Berbigier, P., Bernhofer, C., Buchmann, N., Giulmanov, T., Granier, A., Grünwald, T., Havránková, K., Ilvesniemi, H., Janous, D., Knohl, A., Laurila, T., Lohila, D., Loustau, D., Matteucci, G., Meyers, T., Miglietta, F., Ourcival, J.-M., Pumpanen, J., Rambal, S., Rotenberg, E., Sanz, M., Tenhunen, J., Seufer, G., Vaccari, F., Vesala, T., Yakir, D., Valantini, R., 2005. On the separation of net ecosystem exchange into assimilation and ecosystem respiration: review and improved algorithm. Glob. Change Biol. 11, 1424–1439. https://doi.org/10.1111/j.1365-2486.2005.001002.x.
Rodrigues, T.R., Vourlitis, G.L., Lobo, F.A., Oliveira, R.G., Nogueira, J.S., 2014. Seasonal variation in energy balance and canopy conductance for a tropical savanna ecosystem of south central Mato Grosso, Brazil. J. Geopys. Res.: Biogeosci. 119, 1–13. https://doi.org/10.1002/2013JG002472.
Ropelewski, C.F., Halpert, M.S., 1987. Global and regional scale precipitation patterns associated with the el niño/Southern oscillation. Mon. Weather Rev. 115, 1606–1626.
Sánchez, J.M., Caselles, V., Rubio, E.M., 2010. Analysis of the energy balance closure over a FLUXNET boreal forest in Finland. Hydrol. Earth Syst. Sci. 14, 1487–1497. https://doi.org/10.5194/hess-14-1487-2010.
Santos, A.S., Santos e Silva, C.M., 2013. Seasonality, interannual variability, and linear tendency of wind speeds in the Northeast Brazil from 1986 to 2011. The Sci. World J. 490857. https://doi.org/10.1155/2013/490857.
Santos, R.M., Oliveira-Filho, A.T., Eisenlohr, P.V., Queiroz, L.P., Cardoso, D.B.O.S., Rodal, M.J.N., 2012. Identity and relationships of the Arboreal Caatinga among other floristic units of seasonally dry tropical forests (SDTFs) of north-eastern and Central Brazil. Ecol. Evol. 2 (2), 409–428. https://doi.org/10.1002/ece3.91.
Santos, M.G., Oliveira, M.T., Figueiredo, K.V., Hawk, H.M., Ahmadi, E.C.P., Almeida-Cortez, J., Sampaio, E.V.S.B., Ometto, J.H.B., Menezes, R.C.S., Oliveira, A.F.M., Pompelli, M.F., Antonino, A.C.D., 2014. The Brazilian Caatinga, dry tropical forest: can it tolerate climate changes. Theor. Exp. Plant. Physiol 26, 83–99. https://doi.org/10.1007/s40626-014-0008-0.
Schimel, D.S., House, J.I., Hibbard, K.A., Bousquet, P., Ciais, P., Braswell, B.H., Apps, M.J., Baker, D., Bondeau, A., Canadell, J., Churkina, G., Cramer, W., Denning, A.S., Field, C.B., Friedlingstein, P., Goodale, C., Heimann, M., Houghon, R.A., Melillo, J.M., Moore III, B., Murdiyarso, D., Noble, I., Pacala, S.W., Prentice, I.C., Raupach, M.R., Rayner, P.J., Scholes, R.J., Steffen, W.L., Wirth, C., 2001. Recent patterns and mechanisms of carbon exchange by terrestrial ecosystems. Nature. 414, 169–172.
Silva, P.F., Lima, J.R.S., Antonino, A.C.D., Souza, R., Souza, E.S., Silva, J.R.I., Alves, E.M., 2017. Seasonal patterns of carbon dioxide, water and energy fluxes over the Caatinga and grassland in the semi-arid region of Brazil. J. Arid Environ. 147, 71–82. https://doi.org/10.1016/j.jaridenv.2017.09.0030140-1963.
Sotta, E.D., Veldkamp, E., Sxhwendenmann, L., Guimarães, B.R., Paixão, R.K., Ruivo, M.L.P., Costa, A.C.L., Meir, P., 2007. Effects of an induced drought and soil carbon dioxide (CO_2) efflux and soil CO_2 production in an Eastern Amazonian rainforest, Brazil. Glob. Change Biol. 13, 2218–2229. https://doi.org/10.1111/j.1365-2486.2007.01416.x.
Souza, L.Q., Freitas, A.D.S., Sampaio, E.V.S.B., Moura, P.M., Menezes, R.S.C., 2012. How much nitrogen is fixed by biological symbiosis in tropical dry forest? 1. Trees and shrubs. Nutr. Cycl. Agroecosyst. 94, 171–179.
Souza, R., Feng, X., Antonino, A., Montenegro, S., Souza, E., Porporato, A., 2016. Vegetation response to rainfall seasonality and interannual variability in tropical dry forests. Hydrol. Process. 30, 3582–3595. https://doi.org/10.1002/hyp.10953.
Stoy, P.C., Mauder, M., Foken, T., Marcolla, B., Boegh, E., Ibrom, A., Arain, M.A., Arneth, A., Aurela, M., Bernhofer, C., Cescatti, A., Dellwik, E., Duce, P., Gianelle, D., van Gorsel, E., Kiely, G., Knohl, A., Margolis, H., Mccaughey, H., Merbold, L., Montagnani, L., Papale, D., Reichstein, M., Saunders, M., Serrano-Ortiz, P., Sottocornola, M., Spano, D., Vaccari, F., Varlagin, A., 2013. A data-driven analysis of energy balance closure across FLUXNET research sites: the role of landscape scale heterogeneity. Agric. For. Meteorol. 171–172, 137–152. https://doi.org/10.1016/j.agrformet.2012.11.004.
Sauer, T.J., Horton, R., 2005. Soil heat flux. In: Hartfield, J.L., Baker, J.M. (Eds.), Micrometeorology in Agricultural Systems. ASA Monograph 47, Madison, pp. 131–154. https://doi.org/10.2134/agonmonogr47.c7.
Tavares-Damasceno, J.P., Silveira, J.L.G.S., Câmara, T., Stedile, P.C., Macario, P., Toledo-Lima, G.S., Pichorim, M., 2017. Effect of drought on demography of Pileated Finch (*Coryphospingus pileatus:* Thraupidae) in northeastern Brazil. J. Arid Environ. 147, 63–70. https://doi.org/10.1016/j.jaridenv.2017.09.006.
Teixeira, A.H.C., Bastiaanssen, W.G.M., Ahmad, M.D., Moura, M.S.B., Bos, M.G., 2008. Analysis of energy fluxes and vegetation-atmosphere parameters in irrigated and natural ecosystems of semi-arid Brazil. J. Hydrol. (Amst) 362, 110–127. https://doi.org/10.1016/j.jhydrol.2008.08.011.
Tsuchiya, A., 1995. Preliminary study on the relationship between vessel growth of thorny shrubs and water balance in the semi-arid region, northeastern Brazil. Geog. Sci. 50, 123–131. https://doi.org/10.20630/chirikagaku.50.2_123.
von Randow, C., Manzi, A.O., Kruijt, B., Oliveira, P.J., Zanchi, F.B., Silva, R.L., Hodnett, M.G., Gash, J.H.C., Elbers, J.A., Waterloo, M.J., Cardoso, F.L., Kabat, P., 2004. Comparative measurements and seasonal variations in energy and carbon exchange over forest and pasture in South West Amazonia. Theor. Appl. Climatol. 78, 5–26. https://doi.org/10.1007/s00704-004-0041-z.
von Randow, C., Zeri, M., Restrepo-Coupe, N., Muza, M., Gonçalves, L.G.G., Costa, M.H., Araujo, A.C., Manzi, A.O., da Rocha, H.R., Saleska, S.R., arain, M.A., Baker, I.T., Cestaro, B.P., Cristoffersen, B., Ciais, P., Fisher, J.B., Galbraith, D., Guan, X., van der Hurk, B., Ichii, K., Imbuzeiro, H., Jain, A., Levine, N., Miguez-Macho, G., Poulter, B., Roberti, D., Sahoo, A., Schaefer, K., Shi, M., Tian, H., Verbeeck, H., Yang, Z.-L., 2013. Inter-annual variability carbon and water fluxes in Amazonian, Cerrado and pasture sites, as simulated by terrestrial biosphere models. Agric. For. Meteorol. 182-183, 145–155. https://doi.org/10.1016/j.agrformet.2013.05.015.
Vourlitis, G.L., Nogueira, J.S., Lobo, F.A., Sendall, K.M., Paulo, S.R., Dias, C.A.A., Pinto Jr., O.B., Andrade, N.L.R., 2008. Energy balance and canopy conductance of a tropical semi-deciduous forest of the southern Amazon Basin. Water Resour. Res. 44, W03412. https://doi.org/10.1029/2006WR005526.
Webb, E.K., Pearman, G.I., Leuning, R., 1980. Correction of flux measurements for density effects due to heat and water vapour transfer. Quart. J. Roy. Meteorol. Soc. 106, 85–100.
Wilson, K., Goldstein, A., Falge, E., Aubinet, M., Baldocchi, D., Berbigier, P., Bernhofer, C., Ceulemans, R., Dolman, H., Field, C., Grelle, A., Ibrom, A., Law, B., Kowalski, A., Meyers, T., Moncrieff, J., Monson, R., Oechel, W., Tenhunen, J., Valentini, R., Verma, S., 2002. Energy balance closure at FLUXNET sites. Agric. For. Meteorol. 113, 223–243. https://doi.org/10.1016/S0168-1923(02)00109-0.
Xu, F., Wang, W., Wang, J., Xu, Z., Qi, Y., Wu, Y., 2017. Area-averaged evapotranspiration over a heterogeneous land surface: aggregation of multi-point EC flux measurements with a high-resolution land-cover map and footprint analysis. Hydrol. Earth Syst. Sci. 21, 4037–4051. https://doi.org/10.5194/hess-21-4037-2017.
Zeri, M., Sá, L.D.A., 2010. The impact of data gaps and quality control filtering on the balances of energy and carbon for a Southwest Amazon forest. Agric. For. Meteorol. 150, 1543–1552. https://doi.org/10.1016/j.agrformet.2010.08.004.
Zeri, M., Sá, L.D.A., Manzi, A.O., Araujo, A.C., Aguiar, R.C., von Randow, C., Sampaio, G., Cardoso, F.L., Nobre, C.A., 2014. Variability of carbon and water fluxes following climate extremes over a tropical forest in Southwestern Amazonia. PLoS One 9, e88130. https://doi.org/10.1371/journal.pone.0088130.